Electronic Supplementary Material (ESI) for Organic Chemistry Frontiers.

Twisted Organic TADF Triads based on Diindolocarbazole Donor for Efficient Photoisomerization of Stilbene and Photo-arylation of Heteroarenes

Sushil Sharma[1] and Sanchita Sengupta[1*]

[1]Department of Chemical Sciences, Indian Institute of Science Education and Research (IISER) Mohali, Knowledge City, Sector 81, P.O. Manauli, Mohali, Punjab 140306, India.

*E-mail: sanchita@iisermohali.ac.in

Table of contents

1. Materials and Methods

All chemicals and solvents were purchased from commercial suppliers (Sigma Aldrich, SD Fine Chemicals) and used without further purification. Toluene (Tol) was dried over sodium/benzophenone and distilled prior to use. Silica gel of mesh size 60-120 was used for column chromatography. The ^{1}H and ^{13}C NMR spectra were recorded on a 400 MHz Bruker Biospin Avance III FT-NMR spectrometer, respectively with TMS as standard at room temperature. The solvent used was $CDCl_3$ (from Merck, Germany) and all the spectra were recorded in $CDCl_3$ and dimethyl sulfoxide-d_6 (DMSO) with TMS as the internal standard. Mass spectrometry measurements were performed on UltrafleXtreme MALDI TOF/TOF (Bruker Daltonics) instrument. Software used for acquiring mass spectra was Flex Control, Bruker (USA) and software used for analyzing mass spectra was Flex Analysis 3.1.

All spectroscopic measurements were performed at room temperature unless otherwise mentioned. UV/Vis spectra were recorded on Carey 5000 UV/Vis spectrophotometer using a quartz cuvette with 1 cm path length. Fluorescence solution measurements were performed with Hitachi F7000 fluorescence spectrophotometer equipped with R928F photomultiplier expandable up to 900 nm. Various excitation wavelengths were used to perform the fluorescence measurements. Standard software FL Solutions was used for the measurement and analysis of the data.

Electrochemical measurements were performed using CHI-610E electrochemical workstation from CH Instruments (USA), with a conventional three electrode single-compartment cell consisting of a glassy carbon as the working electrode, Ag/AgCl containing 3M KCl solution as the reference electrode, and Pt wire as the counter electrode. Cyclic voltammetry measurements were performed at a scan-rate of 0.1 V/s. As a supporting electrolyte, 0.1 M tetrabutylammonium hexafluorophosphate (TBAHPF) (Alfa Aesar) dissolved in pre-dried DCM was used. The solutions were purged with nitrogen for 2 mins prior to measurement. The

concentration of the prepared samples was ~ 0.1-0.3 mM. The electrochemical potential was internally calibrated against the standard ferrocene/ferrocenium (Fc/Fc^{+}) redox couple. Time resolved fluorescence spectra were measured using time-correlated single photon counting (TCSPC) model from Fluorocube, Horiba Jobin Yvon, NJ equipped with picosecond laser diodes as excitation source. The 375 nm laser diode was used as a light source for the excitation of samples and the instrument response function (IRF) was collected using Ludox (colloidal silica) solution. The width (FWHM) of IRF was ~ 250 ps. The optical pulse durations from < 70ps were used. Highly integrated picosecond PMT modules as well as microchannel plate PMTs were used for the time resolution.

Photocatalysis were performed using Blue LED light.

Quantum chemical density functional theory (DFT) and TD-DFT calculations were performed for **DI-PF** and **DI-PI** in the ground state and excited state using Gaussian09 program suite.[S1] The side chains in all molecules were replaced with methyl groups in order to account for the electron-donating effect of the alkyl chain and at the same time reduce the computational time and cost. The studied molecules were optimized using a global hybrid B3LYP functional and 6–31G (d, p) basis set. The frontier molecular orbitals (FMO) electronic levels and FMO distributions were obtained from geometry optimization of neutral ground state geometries. In order to achieve theoretical ΔE_{ST}, TD-DFT calculations were performed in chloroform ($CHCl_3$) using the polarization continuum model (PCM), B3LYP functional and 6–31G (d, p) basis set to determine the singlet and triplet energy levels.

2. Synthesis

Synthesis of 10,15-dihydro-5H-diindolo[3,2-a:3',2'-c]carbazole (2):

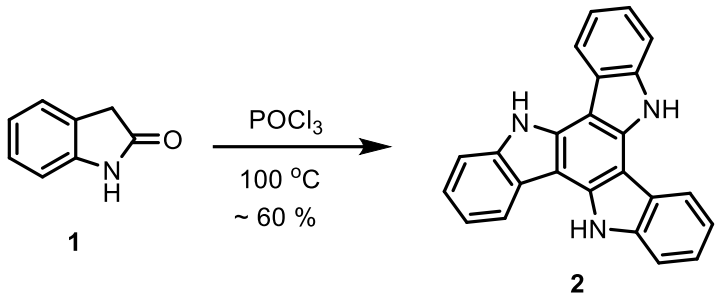

Scheme S1: Synthesis of **2**.[S2]

Procedure: A solution of 2-indolinone (2 g, 15 mmol) in $POCl_3$ (10 mL) was heated at 100 °C for overnight. Then, the reaction mixture was poured into ice and neutralized carefully with KOH. After neutralization, the precipitate was filtered and dried. The compound was separated by column chromatography using ethyl acetate and hexane (20/80, v/v) as eluent. Further, the compound was purified by recrystallization in acetone and hexane mixture to obtain pale-yellow solid with 60 % yield.

^{1}H NMR (400 MHz, DMSO): δ (ppm) 11.88 (s, 3 H), 8.67 (d, J = 8 Hz, 3 H), 7.72 (d, J = 8 Hz, 3 H), 7.41-7.31 (m, 6 H).

5,10-Bis(4-(tert-butyl)phenyl)-10,15-dihydro-5H-diindolo[3,2-a:3',2'-c]carbazole (4):

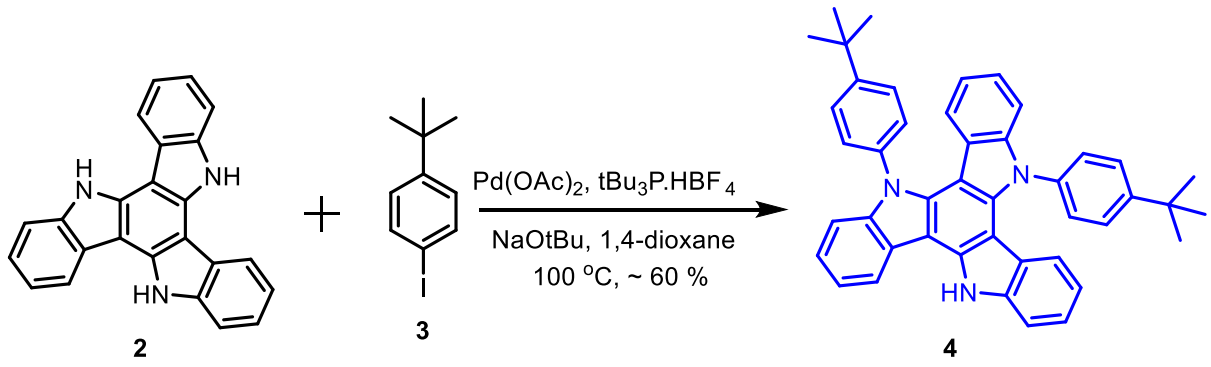

Scheme S2: Synthesis of DI (**4**).[S3]

Procedure: Diindolocarbazole (**2**) (200 mg, 0.579 mmol) and 4-tert-butyliodobenzene (316 mg, 1.216 mmol) were dissolved in 1,4-dioxane and degassed by freeze-pump-thaw method. In a two-neck round bottomed flask, $Pd(OAc)_2$ (5.2 mg, 0.023 mmol), tri-tert-butylphosphine tetrafluoroborate (25 mg, 0.087 mmol) and sodium tert-butoxide (260 mg, 2.316 mmol) were taken and simultaneously 2 and compound 3 were added and heated at 100 °C for 18 h. The

reaction was cooled and diluted with DCM and washed with brine solution. The organic layer was dried over sodium sulphate and concentrated at rotary evaporator. The compound was purified by column chromatography using ethyl acetate and hexane (5/95, v/v) as eluent to obtain an off-white colour solid with 20 % yield.

^{1}H NMR (400 MHz, DMSO): δ 11.95 (s, 1 H), 8.83 (d, J = 8.0 Hz, 1 H), 7.74 (dd, J = 4 Hz, 4 Hz, 4 H), 7.65 (t, J = 8 Hz, 3 H), 7.58 (d, J = 8 Hz, 2 H), 7.49 – 7.37 (m, 3 H), 7.22 – 7.11 (m, 3 H), 6.66 – 6.56 (m, 2 H), 5.76 (d, J = 8 Hz, 1 H), 5.54 (d, J = 8 Hz, 1 H), 1.48 (s, 18 H).

Synthesis of 2,7-dibromophenanthrene-9,10-dione (6):

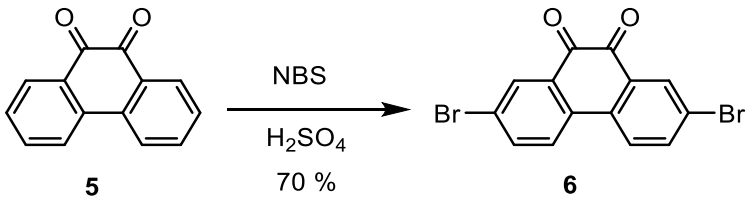

Scheme S3: Synthesis of **6**.[S4]

Procedure: To a solution of phenanthrene-9,10-dione (500 mg, 2.4 mmol) in H_2SO_4 (10 mL), N-bromosuccinimide (NBS) (1 g, 6 mmol) was added while stirring. The reaction mixture was stirred for 3 h at room temperature and then the reaction mixture was poured onto ice. The orange precipitate was filtered out and recrystallized in dimethyl sulfoxide (DMSO) to obtain pure compound as a orange colour solid with 70 % yield.

^{1}H NMR (400 MHz, DMSO): δ (ppm) 8.25 (d, J = 8 Hz, 2 H), 8.08 (d, J = 4 Hz, 2 H), 7.96 (dd, J = 8.4 Hz, 2 H).

2,7-dibromo-11,12-difluorodibenzo[a,c]phenazine (PF):

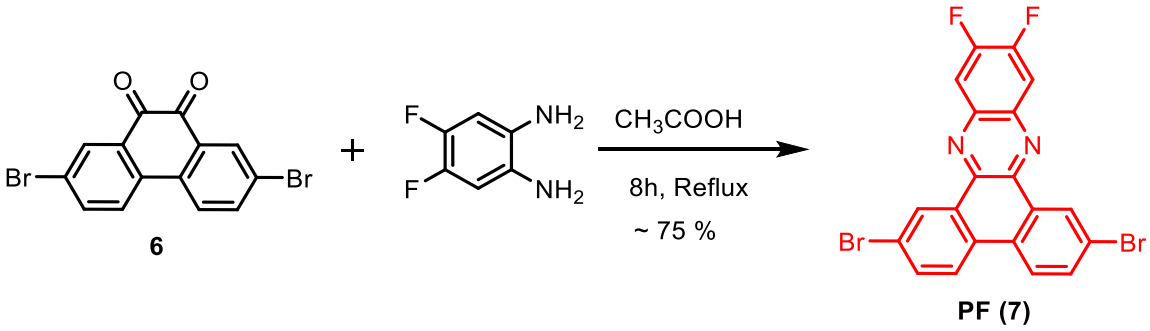

Scheme S4: Synthesis of PF (**7**).[S5]

Procedure: To a solution of dibromophenanthrene-9,10-dione (**6**), (100 mg, 0.273 mmol) in acetic acid, 1,2-Diamino-4,5-difluorobenzene (47mg, 0.327 mmol) was added while stirring and the mixture was refluxed for 8 h. The reaction mixture was stopped, cooled and then poured in ice and then filtered followed by washing with water and methanol afforded greenish solid with 75 % yield.

^{1}H NMR (400 MHz, $CDCl_3$) δ 9.47 (d, J = 2.3 Hz, 2 H), 8.38 (d, J = 8 Hz, 2 H), 8.07 (t, J = 8 Hz, 2 H), 7.91 (dd, J = 4 Hz, 2 H).

Synthesis of PI:

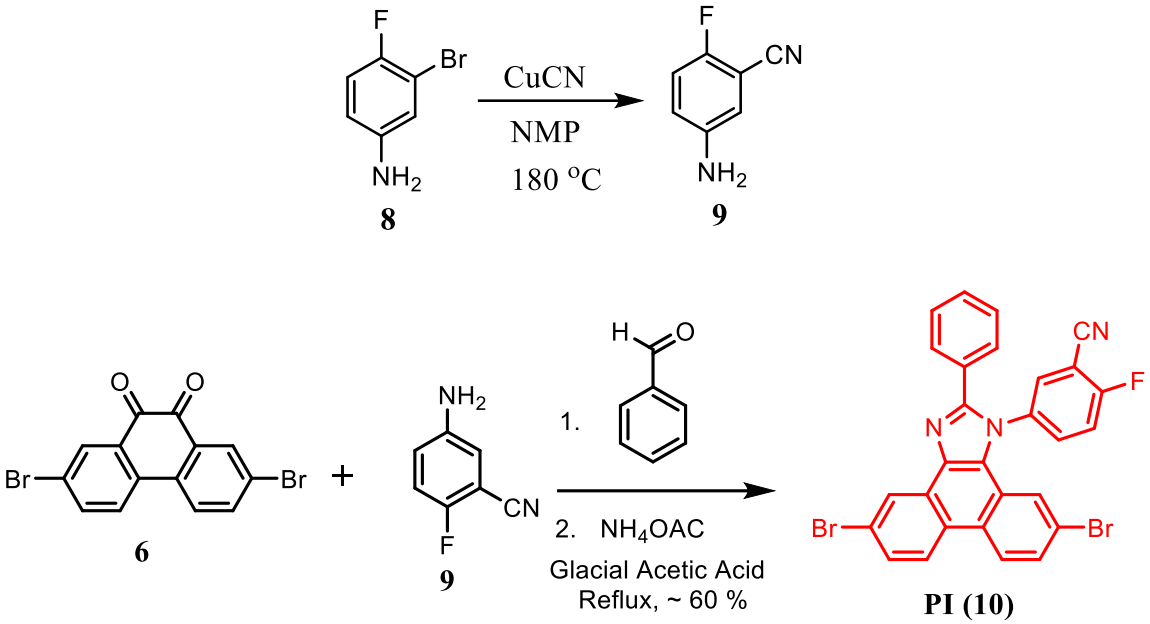

Scheme S5: Synthesis of PI (**10**). [S6]

Procedure: Compound **8** (100 mg, 0.53 mmol) was dissolved in 10 mL NMP and then copper (I) cyanide (71 mg, 0.8 mmol) was added and heated at 150 °C for 3 h. The reaction mixture cooled to room temperature and then water, ammonium hydroxide was added to reaction mixture and stirred for 30 minutes. Then the mixture was extracted three times by ethyl acetate and dried in rotary evaporator. The pure compound was obtained by column chromatography using ethyl acetate and hexane (2/98, v/v) as eluent.

A mixture of compound **6** (100 mg, 0.27 mmol), compound **9** (44 mg, 0.32 mmol), benzaldehyde (29 mg, 0.27mmol) and ammonium acetate (104 mg, 1.35 mmol) in 8 mL glacial acetic acid was refluxed for 14 h. After completion of reaction, the reaction mixture was cooled to room temperature and then added to ice water. The pale-yellow precipitate was formed and

collected by filtration followed by washing with water and methanol to obtain off-white solid with 60 % yield.

^{1}H NMR (400 MHz, DMSO) δ (ppm) 8.86 (d, J = 8.0 Hz, 1 H), 8.80 (d, J = 8 Hz, 1 H), 8.74 (d, J = 4 Hz, 1 H), 8.60 (dd, J = 4 Hz, 4 Hz, 1 H), 8.32 – 8.26 (m, 1 H), 7.95 (t, J = 8 Hz, 1 H), 7.82 (dd, J = 8 Hz, 1 H), 7.74 (dd, J = 8 Hz, 1 H), 7.60 – 7.55 (m, 2 H), 7.43 (d, J = 8 Hz, 3 H), 7.02 (d, J = 4 Hz, 1 H).

Synthesis of DI-PF:

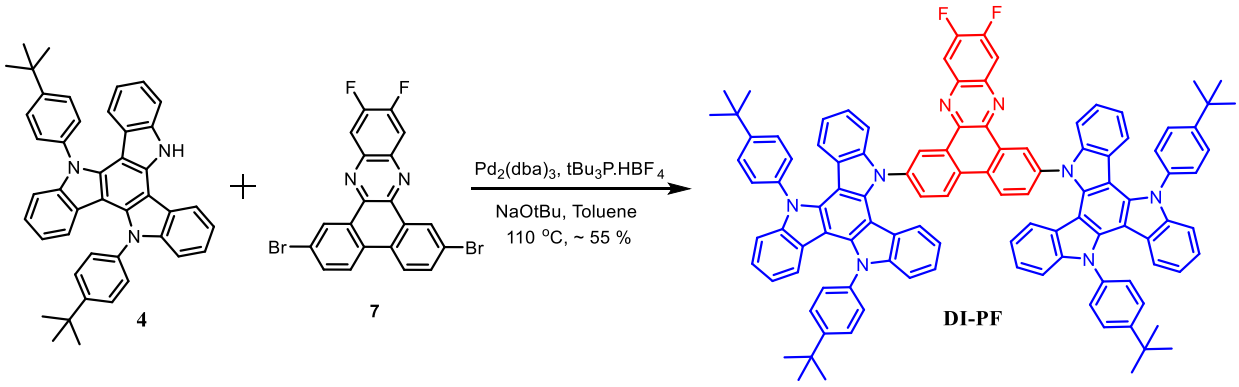

Scheme S6: Synthesis of **DI-PF**. [S7]

Procedure: Compound **4** (50 mg, 0.105 mmol) and compound **7** (160 mg, 0.262 mmol) were dissolved in Tol and degassed by freeze-pump-thaw method. In a two-neck round bottomed flask, $Pd_2(dba)_3$ (5 mg, 0.0053 mmol), tri-tert-butylphosphine tetrafluoroborate (5 mg, 0.016 mmol) and sodium tert-butoxide (50 mg, 0.525 mmol) were taken and simultaneously compound **4** and compound **7** were added and heated at 110 ^{o}C for 12 h. The reaction was cooled and diluted with DCM and washed with brine solution. The organic layer was dried over sodium sulphate and concentrated at rotary evaporator. The compound was purified by column chromatography using chloroform and hexane (10/90, v/v) as eluent to obtain an orange solid with 55 % yield.

^{1}H NMR (400 MHz, $CDCl_3$) δ (ppm) 9.79 (d, J = 2.3 Hz, 2 H), 9.44 (dd, J = 7.9 Hz, 2 H), 8.75 (d, J = 8.8 Hz, 2 H), 8.63 (d, J = 7.3 Hz, 2 H), 8.07 (dd, J = 10.5 Hz, 2 H), 7.94 (ddd, J = 8.3 Hz, 4 H), 7.91 – 7.82 (m, 4 H), 7.67 (s, 6 H), 7.52 (d, J = 7.9 Hz, 2 H), 7.39 (d, J = 7.8 Hz, 2 H), 7.30 (d, J = 8.1 Hz, 2 H), 7.19 (q, J = 7.7 Hz, 4 H), 7.01 (t, J = 7.6 Hz, 2 H), 6.78 – 6.71 (m, 4 H), 6.49 (t, J = 7.0 Hz, 2 H), 6.32 (d, J = 8.1 Hz, 2 H), 5.94 (dd, J = 11.4 Hz, 4 H), 1.51 (s, 18 H), 1.50 (s, 18 H).

^{13}C NMR (100 MHz, $CDCl_3$) δ (ppm) 151.97, 138.24, 138.18, 138.12, 134.79, 131.85, 128.93, 127.04, 127.02, 126.99, 126.96, 126.93, 123.13, 123.09, 122.98, 122.95, 122.89, 122.85,

122.23, 120.14, 120.06, 119.78, 119.64, 110.98, 110.11, 110.00, 109.90, 42.01, 35.14, 31.73, 31.66, 28.59, 26.90, 22.73, 14.22.

ESI-TOF: $(M+H)^+$ of molecular formula $C_{108}H_{84}F_2N_8$: Calculated 1531.6878; found 1531.6588.

Synthesis of DI-PI:

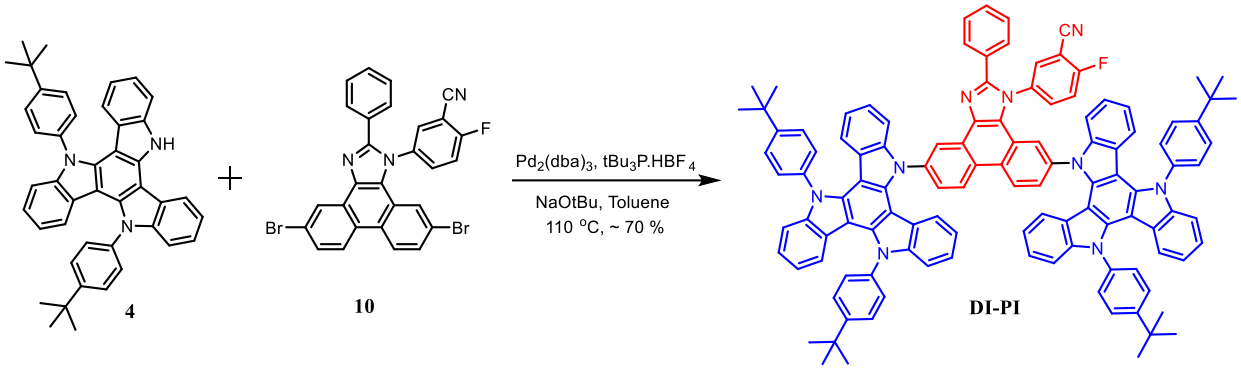

Scheme S7: Synthesis of **DI-PI**.[S7]

Procedure: Compound **4** (122 mg, 0.2 mmol) and compound **10** (50 mg, 0.087 mmol) were dissolved in Tol and degassed by freeze-pump-thaw method. In a two-neck round bottomed flask, $Pd_2(dba)_3$ (4 mg, 0.004 mmol), tri-tert-butylphosphine tetrafluoroborate (4 mg, 0.013 mmol) and sodium tert-butoxide (42 mg, 0.435 mmol) were taken and simultaneously compound **4** and compound **10** were added and heated at 110 °C for 12 h. The reaction was cooled and diluted with DCM and washed with brine solution. The organic layer was dried over sodium sulphate and concentrated at rotary evaporator. The compound was purified by column chromatography using chloroform and hexane (10/90, v/v) as eluent to obtain off-white solid with 70 % yield.

^{1}H NMR (400 MHz, DMSO) δ (ppm) 11.94 (s, 2 H), 8.83 (d, J = 4 Hz, 2 H), 7.74 (dd, J = 4 Hz, 11 H), 7.71 – 7.60 (m, 9 H), 7.58 (d, J = 8 Hz, 5 H), 7.49 – 7.37 (m, 8 H), 7.22 – 7.11 (m, 8 H), 6.66 – 6.56 (m, 5 H), 5.76 (d, J = 8.1 Hz, 2 H), 5.55 (d, J = 8.1 Hz, 2 H), 1.47 (s, 36 H).

^{13}C NMR (101 MHz, DMSO) δ (ppm) 151.69, 151.55, 140.80, 139.30, 137.53, 137.27, 136.05, 134.68, 128.71, 128.32, 126.95, 123.62, 122.90, 122.34, 121.62, 121.34, 120.61, 120.16, 119.41, 110.81, 110.15, 109.50, 102.69, 102.04, 34.76, 31.30.

ESI-TOF: $(M-C_{13}H_8FN-2H)^-$ of molecular formula $C_{103}H_{82}N_8$: Calculated 1428.6486; found 1428.6592.

3. ^{1}H and ^{13}C NMR spectra

^{1}H NMR spectra of 2

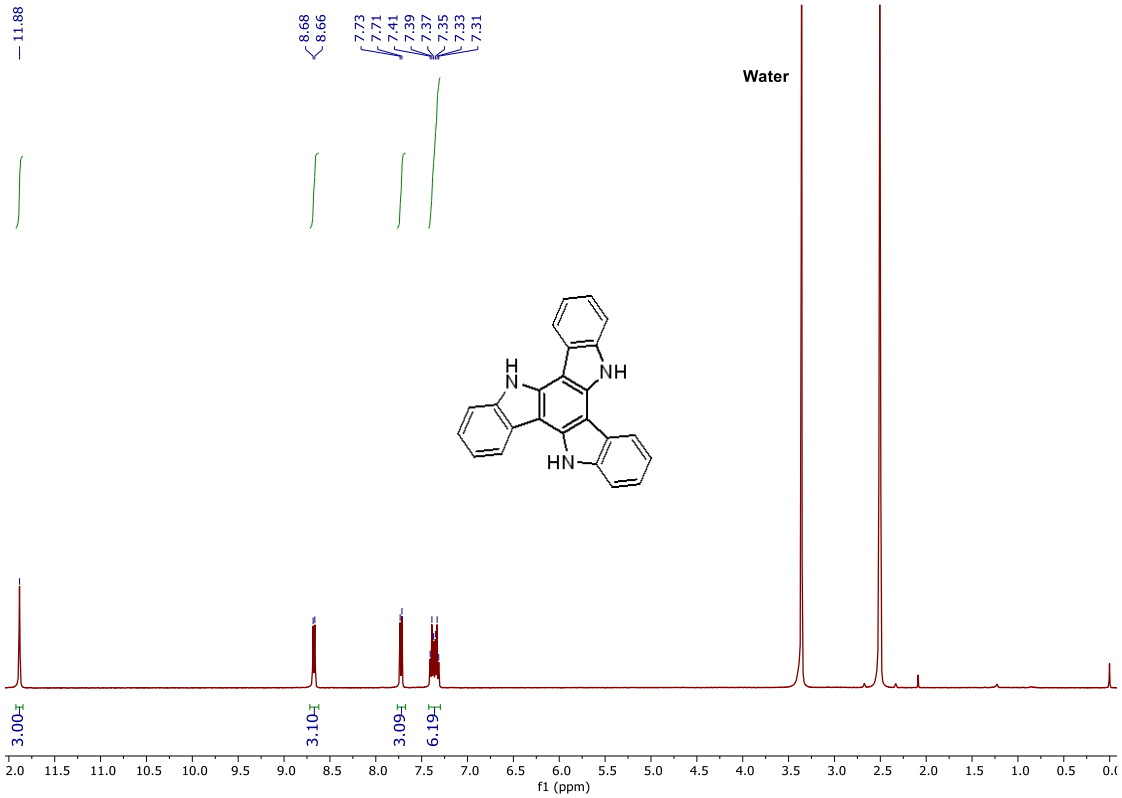

^{1}H NMR spectra of DI

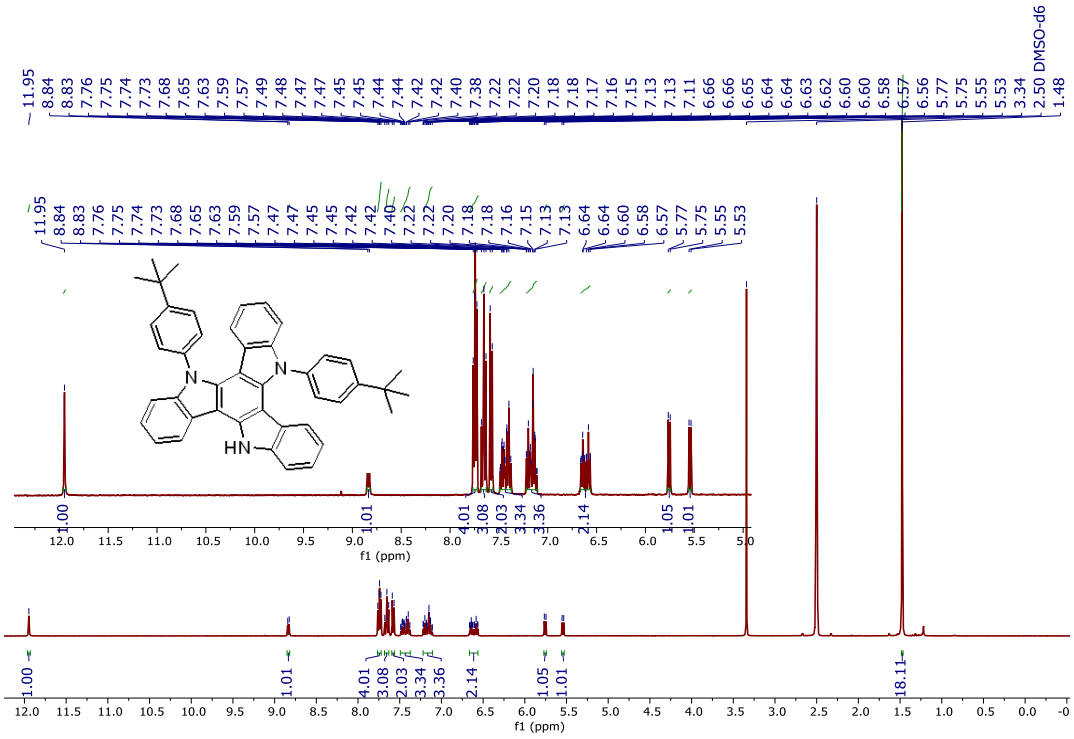

^{1}H NMR spectra of 6

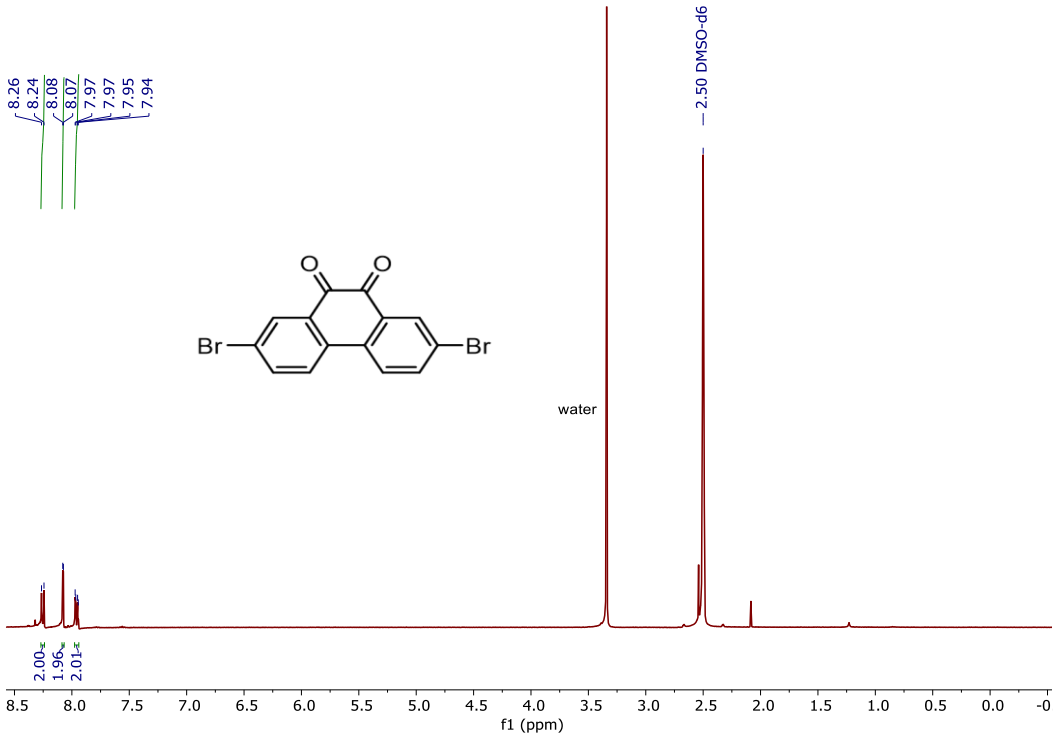

^{1}H NMR spectra of PF

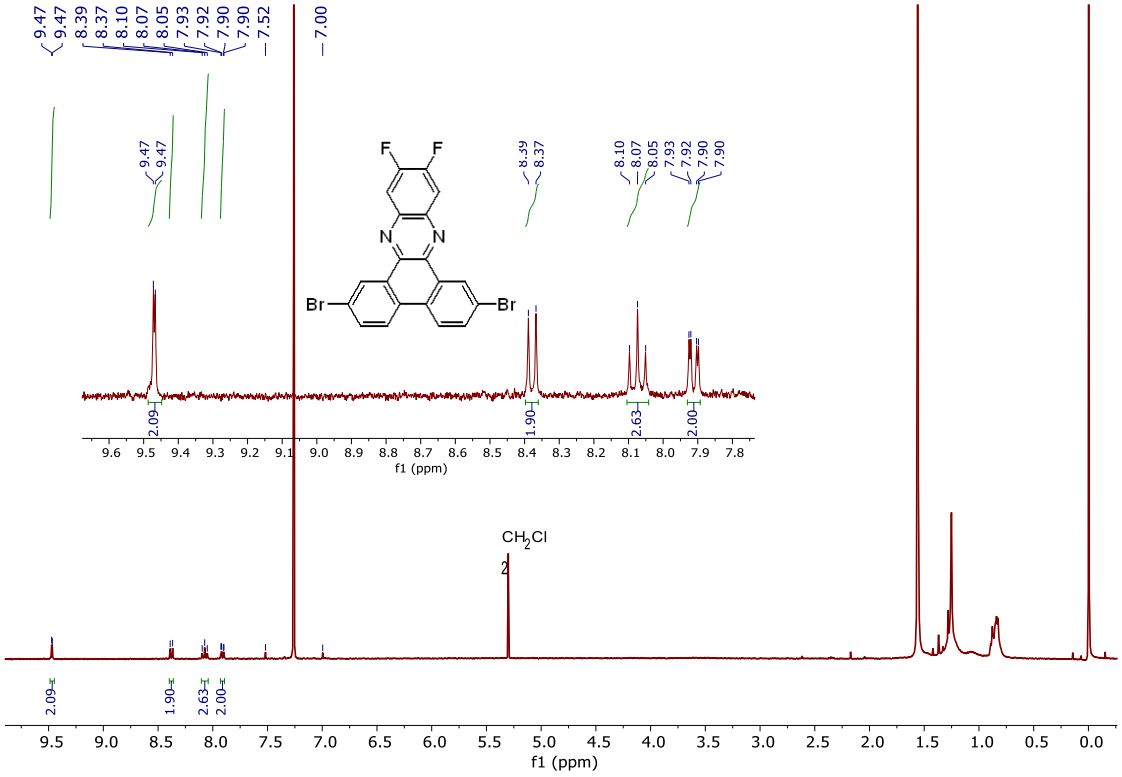

^{1}H NMR spectra of PI

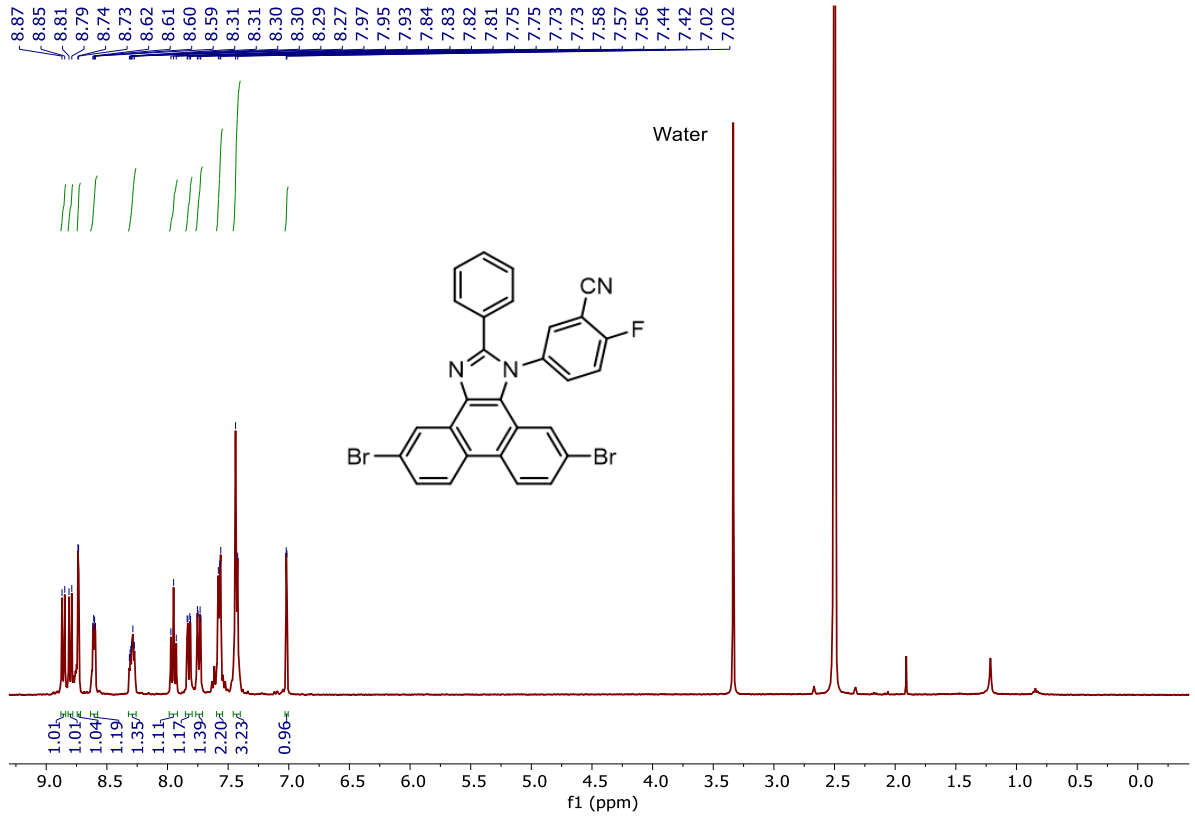

^{1}H NMR spectra of DI-PF

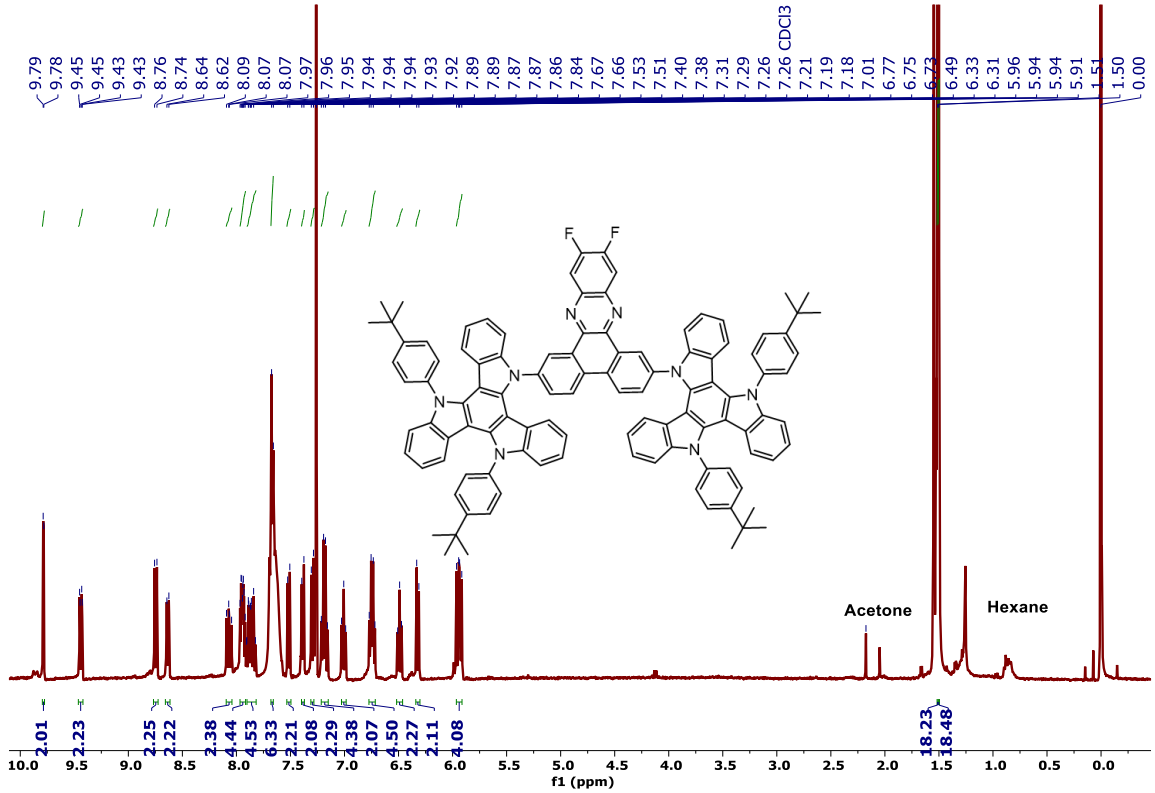

^{13}C NMR spectra of DI-PF

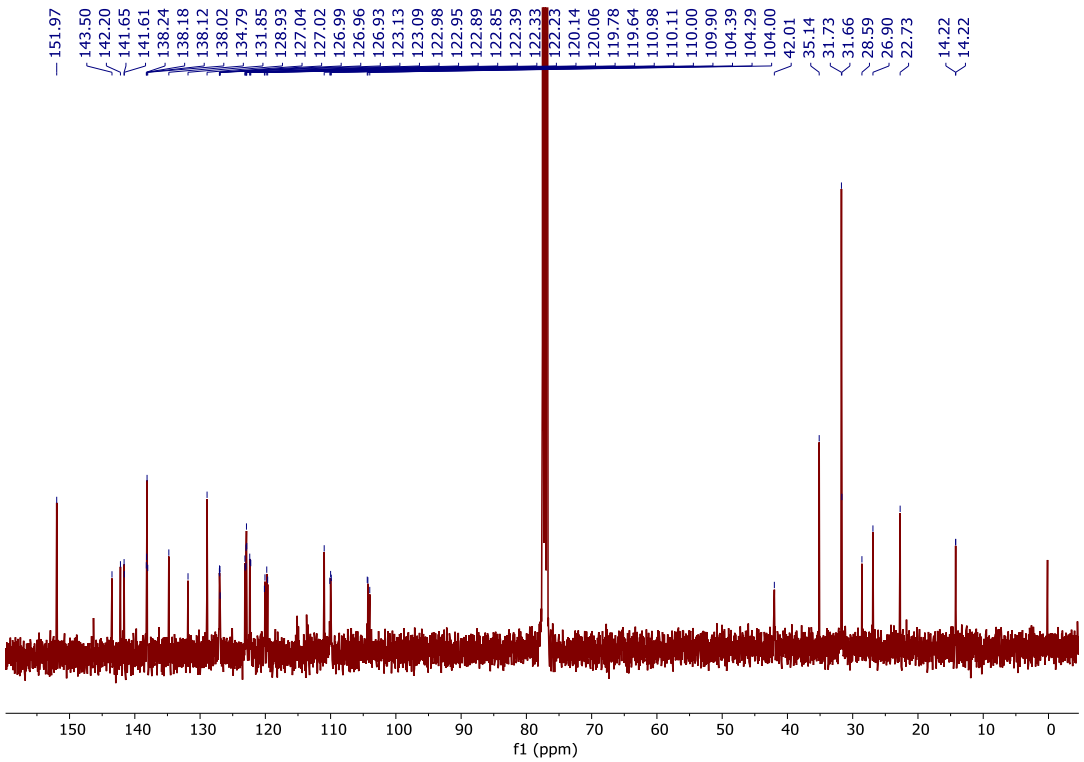

^{1}H NMR spectra of DI-PI

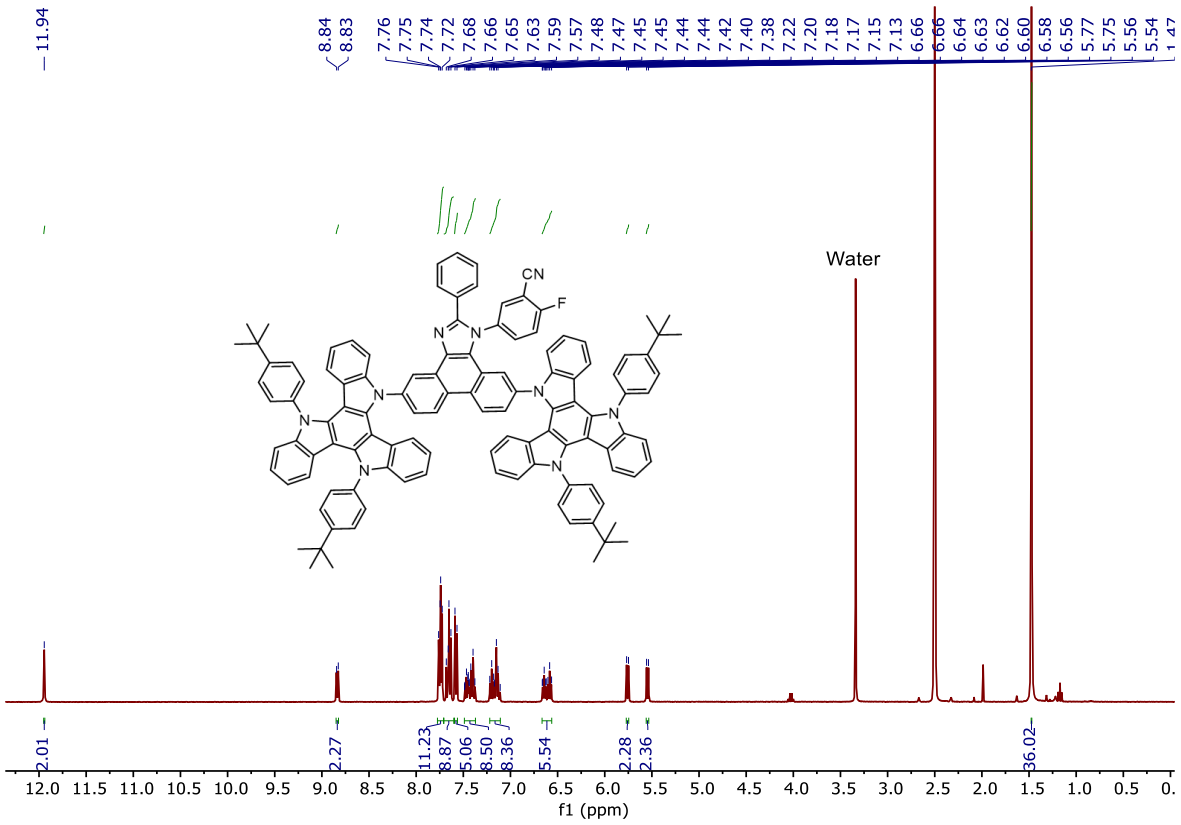

^{13}C NMR spectra of DI-PI

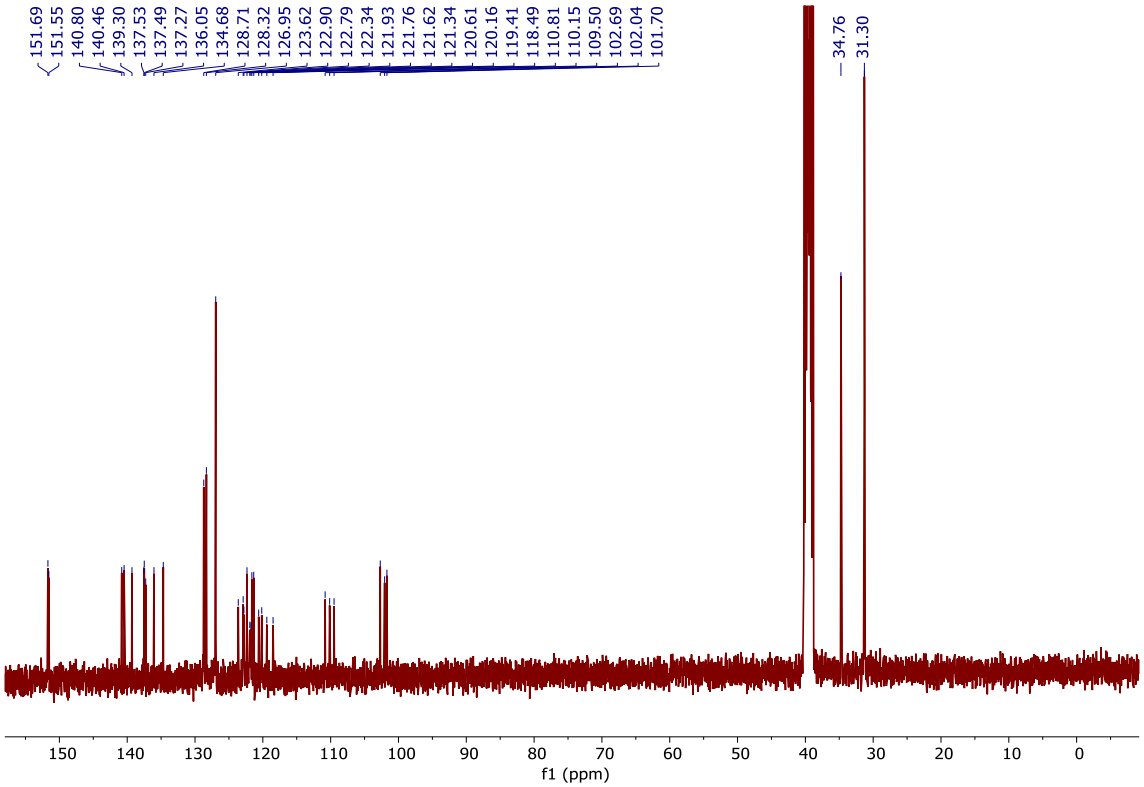

4. Photophysical Characterization

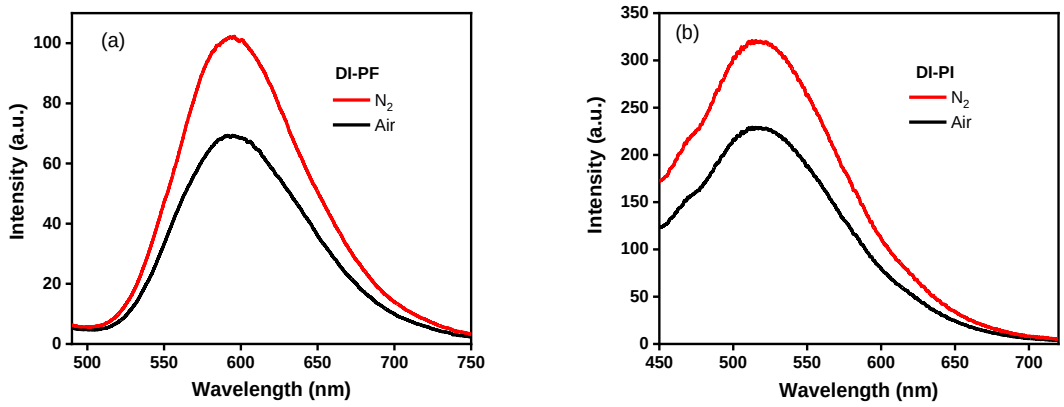

Figure S1. Emission spectra of (a) **DI-PF** and (d) **DI-PI** in aerated solution and nitrogen degassed solution of Tol and $CHCl_3$ upon excitation at 394 nm and 393 nm respectively.

5. Density Functional Theory (DFT) Calculations

To determine the electronic properties of **DI-PF** and **DI-PI**, DFT calculations were performed for optimized structure and time dependent DFT (TD-DFT) for energy calculations using the Gaussian 09 package at the B3LYP/6-31G(d,p) level. Due to large steric hindrance between donor and acceptor, **DI-PF** and **DI-PI** showed large twist angle of 65.7˚and 66.3˚ respectively.

Therefore, highest occupied molecular orbital (HOMO) completely localized on donor part and lowest unoccupied molecular orbital (LUMO) completely localized on acceptor part as shown in Figure S2. Such separations of HOMO and LUMO level leads to a small ΔE_{ST} for better TADF performances. The singlet and triplet energy levels were 2.078 eV and 2.025 eV for **DI-PF** and 2.595 eV and 2.591 eV for **DI-PI** respectively calculated by TD-DFT method. The discrepancies in experimentally and theoretically calculated studies might occur due to the limitations in the theoretical models as well as the fact the experimental results were observed at 77K.[S8]

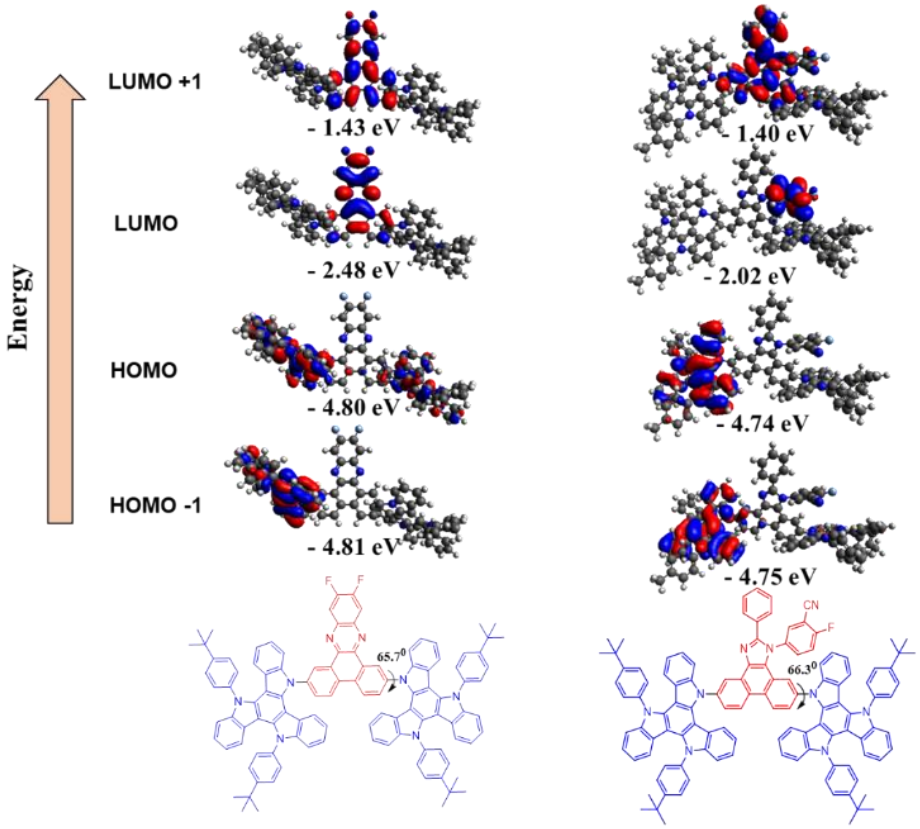

Figure S2. Geometry optimization and FMO energy levels of **DI-PF** and **DI-PI** calculated using B3LYP/6-31G(d, p) and singlet and triplet energy diagram of **DI-PF** and **DI-PI.**

Table S1. FMO energy levels and dihedral angles of compounds **DI-PF** and **DI-PI** calculated by B3LYP/6-31G(d,p).

Compound	HOMO-1 (eV)	HOMO (eV)	LUMO (eV)	LUMO+1 (eV)	Dihedral angle (°)
DI-PF	- 4.81	- 4.80	- 2.48	- 1.43	65.7

DI-PI	- 4.75	- 4.74	- 2.02	- 1.40	66.3

6. Low Temperature Fluorescence and Phosphorescence

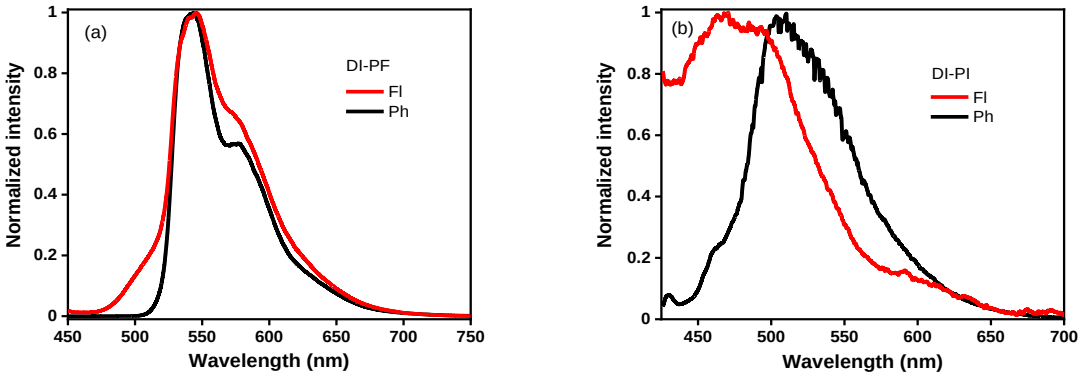

Figure S3. Low temperature (77 K) fluorescence and phosphorescence of (a) **DI-PF** in Tol and (b) **DI-PI** in $CHCl_3$ ($c \sim 10^{-6}$ M) upon excitation at 394 nm and 393 nm respectively at 77 K.

7. Solvatochromism

The peaks observed in long wavelength region might be attributed to CT, hence solvatochromic study was performed for **DI-PF** and **DI-PI** in solvents of different polarities and in binary mixture of methylcyclohexane (MCH) and $CHCl_3$. In case of **DI-PF**, in polar solvents such as $CHCl_3$, dichloromethane (DCM) and tetrahydrofuran (THF), the long wavelength peak was not observed due to rapid non-radiative deactivation as shown in Figure S4. While in non-polar solvents such as Tol and MCH, the emission was observed at 593 nm and 528 nm respectively. In case of binary mixture of MCH and $CHCl_3$, the long wavelength peak was not observed upto 60 % of MCH in $CHCl_3$ (v/v). With further increase of MCH percentage of from 60 % to higher, enhancement of emission intensity was observed with hypsochromic shift of the emission maximum by 110 nm.

In case of **DI-PI**, in non-polar solvents (Tol and MCH), only an emission peak was observed at 440 nm, the long wavelength peak was not observed while in polar solvents DCM and THF, along with peak around 440 nm, a shoulder was observed around 510 nm. In $CHCl_3$, the emission peak was obtained at 519 nm. In case of binary mixture of MCH and $CHCl_3$, hypsochromic shift of 58 nm was obtained with the increasing percentage of MCH from 0 % to 90 % as shown in Figure S4. Hence, positive solvatochromism was observed for both compounds which indicates the long wavelength peak was due to CT.

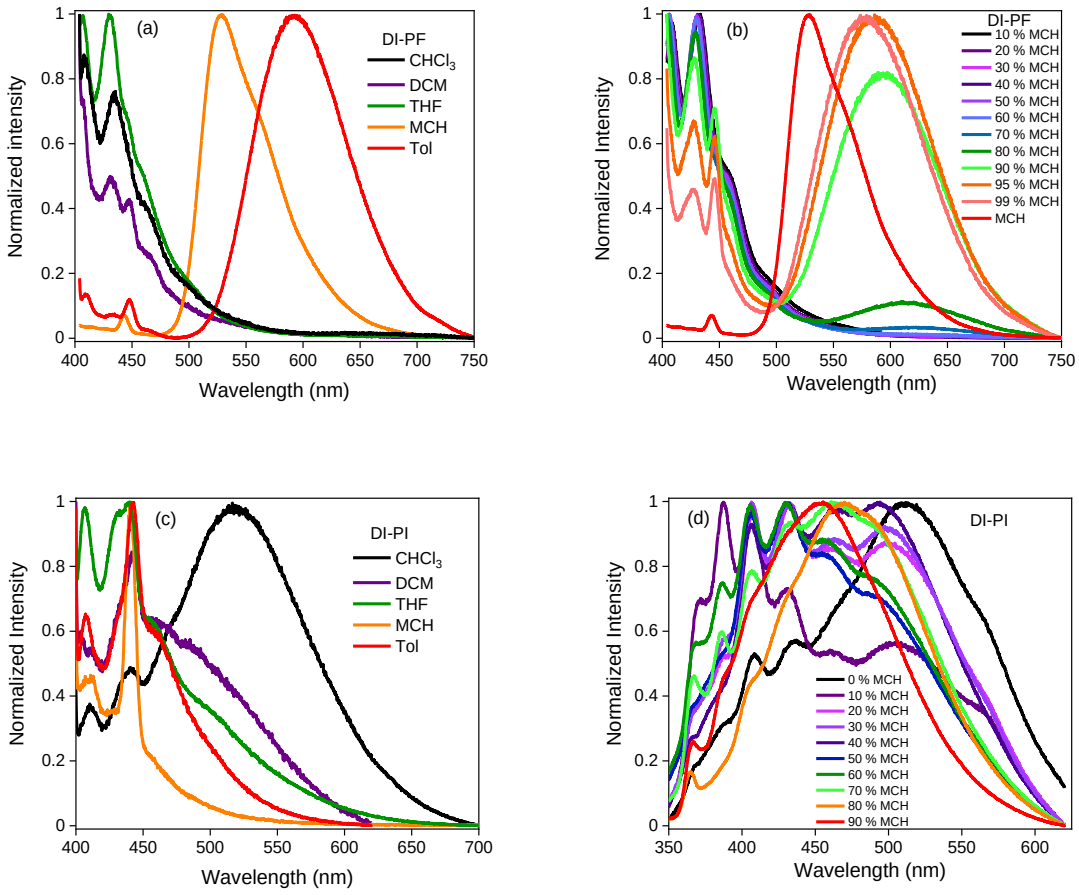

Figure S4. Normalized fluorescence emission spectra of **DI-PF** (a) in solvents of different polarities and (b) in different MCH/$CHCl_3$ (v/v) solvent mixtures and of **DI-PI** (c) in solvents of different polarity and (d) in different MCH/$CHCl_3$ (v/v) solvent mixtures upon excitation at 394 nm and 393 nm respectively.

Table S2. Emission maxima wavelengths of **DI-PF** and **DI-PI** in various solvents.

Compound	MCH	Tol	THF	DCM	$CHCl_3$
DI-PF	528	593	-	-	-
DI-PI	-	-	510	510	519

8. Fluorescence Lifetime

The fluorescence lifetimes were recorded using thin films of 0.5 wt % of **DI-PF** and **DI-PI** with ZEONEX on quartz substrates. The compounds were dried and dissolved in Tol with ZEONEX prior to making thin films, which were drop casted under a nitrogen atmosphere. The transient photoluminescence decay of thin films showed prompt and delayed components and their calculated lifetimes are given in Table S3.

Table S3. Fluorescence lifetime in 0.5 wt % of ZEONEX of **DI-PF** and **DI-PI**.

Compound	Lifetime (Thin films)	
	Prompt (ns)	Delayed (μs)
DI-PF	40	6.15
DI-PI	13.5	2.05

9. Fluorescence Quantum Yield

Fluorescence quantum yields were measured by relative method using Rhodamine B (Φ_R = 0.5 in ethanol (EtOH)) as reference dyes and using the following equation:[S9]

$$\mathbf{\Phi = \Phi_R\,(I/I_R)\,(A_R/A)\,(\lambda_{exR}/\lambda_{ex})\,(n^2/n^2_R)}$$

where Φ_R is the quantum yield of reference dye Rhodamine B in EtOH, I and I_R are integrated fluorescence intensities of compounds and reference dye respectively, A and A_R are the absorbance of the compounds and reference dye respectively, and n and n_R are the refractive indices of solvent(s) used for compounds and reference respectively. The compounds **DI-PF** and **DI-PI** were dissolved in Tol and $CHCl_3$ respectively in three different concentrations (c ~ 10^{-5}-10^{-6} M) such that their absorbance was less than or equal to 0.1 and their absorption and fluorescence spectra were recorded in aerated and nitrogen degassed solution. Absorbance and fluorescence spectra were recorded for three different concentrations of Rhodamine B in EtOH (c ~ 10^{-5}-10^{-6} M). Fluorescence quantum yields were then calculated using the above equation for each compound in aerated solution and degassed solution and the values are given in Table S4 and S5.

Table S4. Relative quantum yields of **DI-PF** and **DI-PI** using relative method and Rhodamine B as a reference dye in aerated solution.

Compound	Absorbance			Integrated Fluorescence Intensity			Quantum Yield $\Phi=\Phi_R(I/I_R)(A_R/A)(\lambda_{exR}/\lambda_{ex})(n^2/n^2_R)$	
	1	2	3	1	2	3	Φ_i	Φ_{avg}
DI-PF	0.066	0.074	0.097	12.74	13.26	15.63	2.5	
							2.6	2.5
							2.4	

DI-PI	0.071	0.092	0.112	22.93	25.18	28.67	4.2	
							4.0	4.0
							3.8	
Rhodamine B (EtOH)	0.033	0.065	0.105	234.7	418.24	655.36	50 (reported value)	

Table S5. Relative quantum yields of **DI-PF** and **DI-PI** using relative method and Rhodamine B as a reference dye in N_2 degassed solution.

Compound	**Absorbance**			**Integrated Fluorescence Intensity**			**Quantum Yield $\Phi=\Phi_R(I/I_R)(A_R/A)(\lambda_{exR}/\lambda_{ex})(n^2/n^2_R)$ (%)**	
	1	**2**	**3**	**1**	**2**	**3**	**Φ_i**	**Φ_{avg}**
DI-PF	0.066	0.074	0.097	18.814	32.817	35.985	3.7	
							6.4	5.2
							5.6	
DI-PI	0.071	0.092	0.112	30.537	37.99	46.408	5.6	
							6.0	6.0
							6.3	
Rhodamine B (EtOH)	0.033	0.065	0.105	234.7	418.24	655.36	50 (reported value)	

10. Cyclic Voltammetry

The redox properties and HOMO and LUMO energy levels of **DI-PF** and **DI-PI** were measured using cyclic voltammetry (CV) in dry dichloromethane (DCM) with 0.1 M tetrabutylammonium hexafluorophosphate as supporting electrolyte and Ag/AgCl as reference electrode. Based on the first oxidation potential onset (E_{onset}^{ox}) and first reduction potential (E_{onset}^{red}), the HOMO and LUMO were calculated[S6] as,

$$\text{HOMO} = -(E_{onset}^{ox} + 4.76)\ \text{eV, and}$$

$$\text{LUMO} = -(E_{onset}^{red} + 4.76)\ \text{eV}$$

Accordingly, the calculated HOMO energies for **DI-PF** and **DI-PI** are -5.49 eV and -5.48 eV respectively and LUMO energies are -3.98 eV and -4.03 eV respectively. Furthermore, to check

their potential applications in photocatalysis reactions, the excited state oxidation potential (E^*_{ox}) and reduction potential (E^*_{red}) were calculated using the following equations:[S10]

$$E^*_{ox} = E_{ox} - E_{0,0},$$

$$E^*_{red} = E_{red} + E_{0,0}$$

where, E_{ox} and E_{red} is the half oxidation potential and half reduction potential respectively and $E_{0,0}$ is the energy of the S_0 to S_1 excited state and calculated by taking the interaction point of normalized absorption and normalized emission spectra. The calculated excited state potentials showed wider redox potential window that can be utilized in photocatalysis.

11. Photocatalysis:

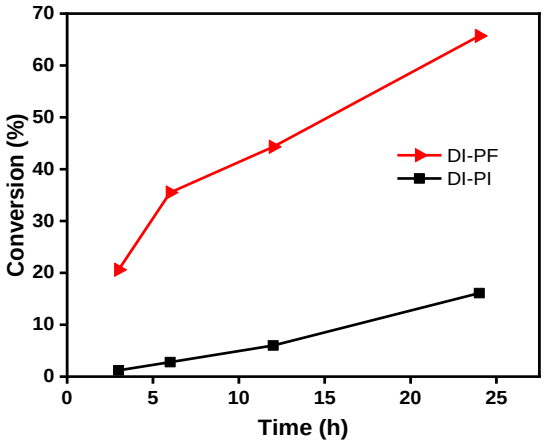

Figure S5. Conversion of E-stilbene to Z-stilbene using **DI-PF** and **DI-PI** as photocatalysts at room temperature in ACN under blue light irradiation.

Table S6. Conversion of E-stilbene to Z-stilbene using **DI-PF** and **DI-PI** as photocatalyst.

Photocatalyst	**Conversion (%)[a]**			
	3 h	**6 h**	**12 h**	**24 h**
DI-PF	21	36	44	66
DI-PI	1.2	3	6	16

[a]Conversion % was calculated by ^{1}H-NMR.

Table S7. Control experiments of Conversion of E-stilbene to Z-stilbene using **DI-PF** as photocatalyst.

Entry	**Conditions**	**Conversion (%)**

1	No light	0
2	No photocatalyst	0

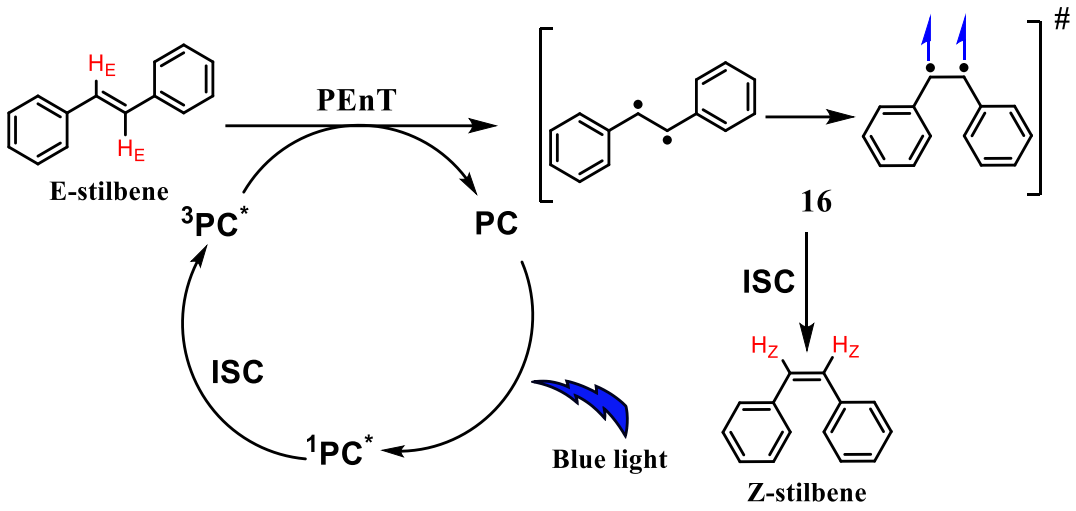

Scheme S8. Plausible mechanistic pathway of photocatalytic isomerization of stilbene.[S10]

^{1}H-NMR spectra of isomerization of stilbene using DI-PF as PC

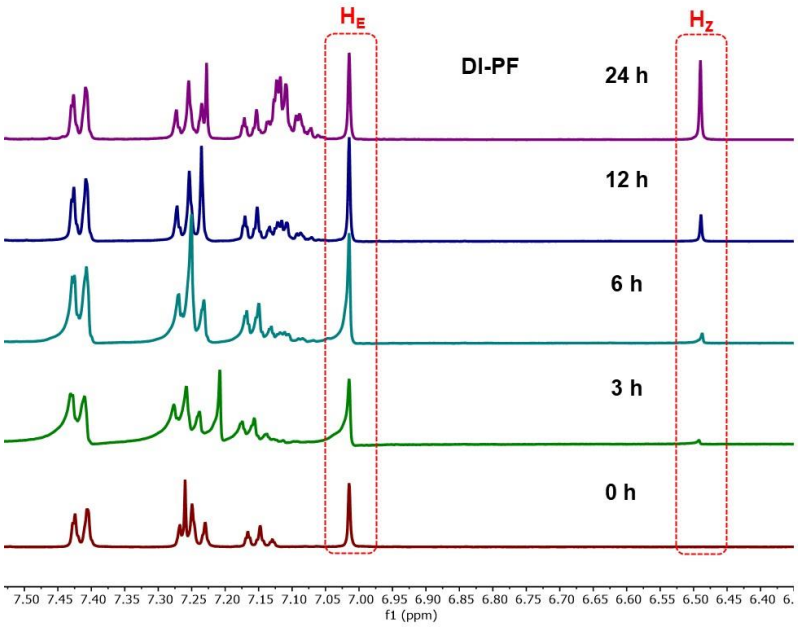

^{1}H-NMR spectra of isomerization of stilbene using DI-PI as PC

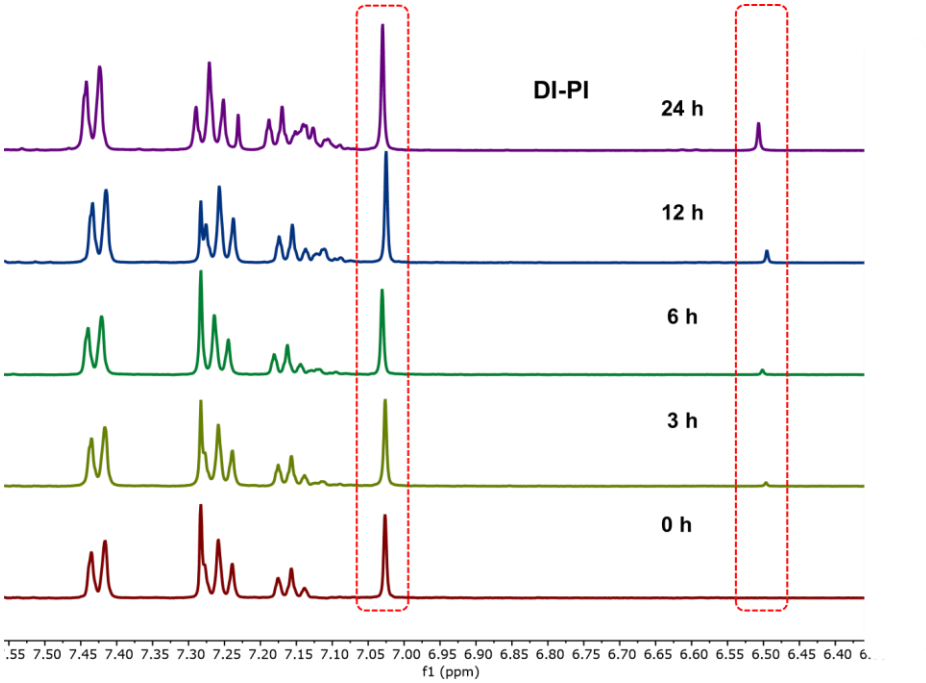

Synthesis:

General procedure for the preparation of aryl diazonium tetrafluoroborates[S11]

To the solution of appropriate aniline (5 mmol) in 2 mL distilled water 50 % hydrofluoroboric acid (1.5 mL) was added and then after cooling the reaction mixture at 0° C, sodium nitrite (0.35 g in 1 mL water) solution was added dropwise in 5 min. interval of time. The reaction mixture was stirred for 30-40 minutes at same temperature and then the formed precipitate was collected by filtration. The precipitate was re-dissolved in minimum amount of acetone and then diethyl ether was added to the solution until the formation of precipitation of diazonium salt. The formed precipitate was washed several times by diethyl ether and dried under vacuum.

Synthesis scheme of 1a:

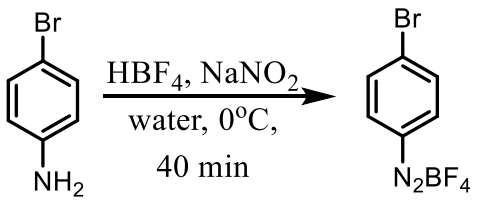

1a

^{1}H NMR (400 MHz, $CDCl_3$): δ (ppm) 8.58 (d, J = 9.0 Hz, 2 H), 8.26 (d, J = 9.0 Hz, 2 H).

Synthesis scheme of 1b:

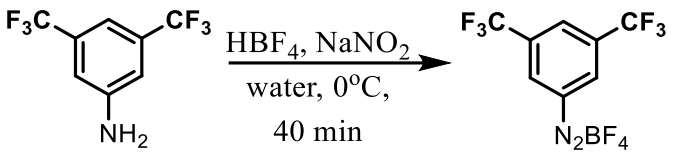

1b

^{1}H NMR (400 MHz, DMSO-*d*$_6$) δ (ppm) 9.51 (s, 2 H), 9.18 (s, 1 H).

Synthesis scheme of 1c:

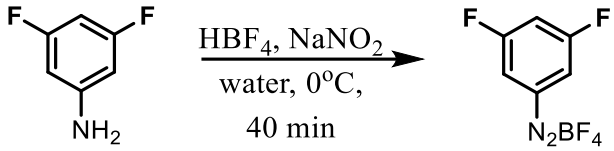

1c

^{1}H NMR (400 MHz, DMSO-*d*$_6$) δ (ppm) 8.64 (dd, *J* = 5.7, 2.4 Hz, 2 H), 8.44 (tt, *J* = 8 Hz, 2.4 Hz, 1 H).

Synthesis scheme of 1-methyl indole (1d):

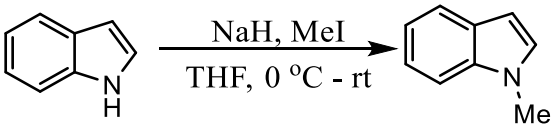

1d

Procedure: Sodium hydride (60% in mineral oil, 15 mmol, 1.5 equiv) was added to a solution of indole (10 mmol, 1.0 equiv) in THF at 0 ℃ and then the reaction mixture was allowed to room temperature and stirred for 30 minutes. Subsequently, the reaction mixture was again cooled to 0 ℃ and methyl iodide (12 mmol, 1.2 equiv) was added dropwise and then reaction mixture was stirred at room temperature until the reaction was completed. After monitoring by TLC, the reaction mixture was cooled to 0 ℃ and quenched with saturated ammonium chloride solution and extracted by diethyl ether. The compound was purified by column chromatography using ethyl acetate and hexane (10/90, v/v) as eluent to obtain an oily compound with 90 % yield.

^{1}H NMR (400 MHz, CDCl$_3$) δ (ppm) 7.73 (d, *J* = 7.9 Hz, 1 H), 7.43 – 7.38 (m, 1 H), 7.35 – 7.29 (m, 1 H), 7.20 (td, *J* = 7.5 Hz, 7.1 Hz, 1.0 Hz, 1 H), 7.11 (d, *J* = 3.1 Hz, 1 H), 6.59 – 6.56 (m, 1 H), 3.83 (s, 3 H).

General procedure for the reaction of aryl diazonium tetrafluoroborates with heteroarenes

The compounds aryl diazonium tetrafluoroborate (1 equiv), photocatalyst (0.01 equiv) and thiphene or furan (5 equiv) were dissolved in dry ACN in a Schlenk tube and the resulting mixture was degassed by freeze-pump-thaw method. The reaction mixture was irradiated by blue LED light and stirred at room temperature for 2 h in N_2 atmosphere. Then the reaction mixture was diluted with ethyl acetate and washed with brine solution. The organic layer was dried over sodium sulphate and concentrated at rotary evaporator. The compound was purified by column chromatography using *n*-hexane as eluent.

2-(4-bromophenyl)thiophene (1P):

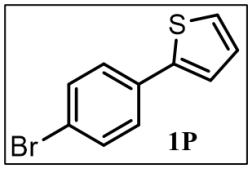

^{1}H NMR (400 MHz, $CDCl_3$) δ (ppm) 7.51 (d, J = 4 Hz, 4 H), 7.32 (d, J = 4 Hz, 2 H), 7.11 (t, J = 4 Hz, 1 H).

2-(3,5-bis(trifluoromethyl)phenyl)thiophene (2P):

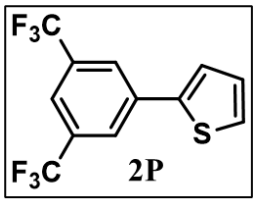

^{1}H NMR (400 MHz, $CDCl_3$) δ (ppm) 8.00 (s, 2 H), 7.77 (s, 1 H), 7.43 (dd, J = 8, 4 Hz, 2 H), 7.15 (t, J = 4 Hz, 1 H).

2-(3,5-difluorophenyl)thiophene (3P):

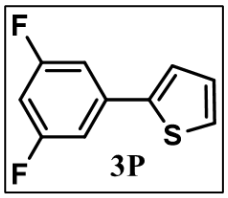

^{1}H NMR (400 MHz, $CDCl_3$) δ (ppm) 7.34 (t, J = 4 Hz, 2 H), 7.11 (t, J = 8 Hz, 3 H), 6.72 (t, J = 8 Hz, 1 H).

2-(4-bromophenyl)furan (4P):

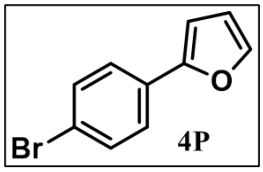

^{1}H NMR (400 MHz, $CDCl_3$) δ (ppm) 7.52 (q, *J* = 8 Hz, 4 H), 7.47 (m, *J* = 4 Hz, 1 H), 6.65 (d, *J* = 4 Hz, 1 H), 6.48 (dd, *J* = 4 Hz, 1 H).

2-(4-bromophenyl)thieno[3,2-b]thiophene (5P):

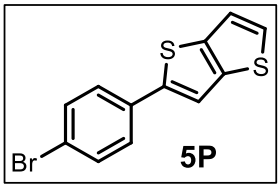

^{1}H NMR (400 MHz, CD_2Cl_2) δ (ppm)7.53 (s, 5 H), 7.42 (d, *J* = 5.0 Hz, 1 H), 7.28 (d, *J* = 4.8 Hz, 1 H).

2-(3,5-bis(trifluoromethyl)phenyl)thieno[3,2-b]thiophene (6P):

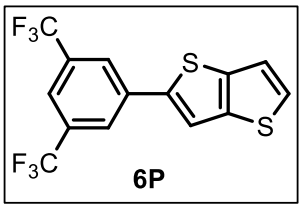

1H NMR (400 MHz, CD_2Cl_2) δ (ppm) 8.01 (s, 2 H), 7.78 (s, 1 H), 7.64 (s, 1 H), 7.49 – 7.43 (m, 1 H), 7.29 (d, *J* = 4.7 Hz, 1 H).

3-(4-bromophenyl)-1-methyl-1H-indole (7P):

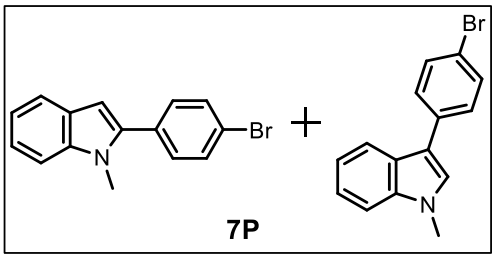

^{1}H NMR (400 MHz, CD_2Cl_2) δ (ppm) 8.63 (d, *J* = 8 Hz, 1 H), 7.63 (dd, *J* = 12, 8 Hz, 3 H), 7.50 (dd, *J* = 12, 8 Hz, 6 H), 7.37 (dt, *J* = 12, 8 Hz, 4 H), 7.25 – 7.17 (m, 3 H), 6.57 (d, *J* = 8 Hz, 1 H), 3.96 (s, 3 H), 3.85 (s, 3 H).

TEMPO Adducts (8P and 9P):

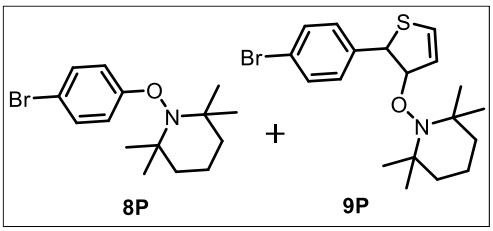

HRMS (ESI): Calculated for **8P**: 312.0962; found: 312.1136 and calculated for **9P**: 396.0996; found: 396.2120.

In the recycling process following the initial cycle, the PCs were purified using column chromatography. Subsequently, these purified and dried PCs were employed for another batch of photocatalysis reactions.

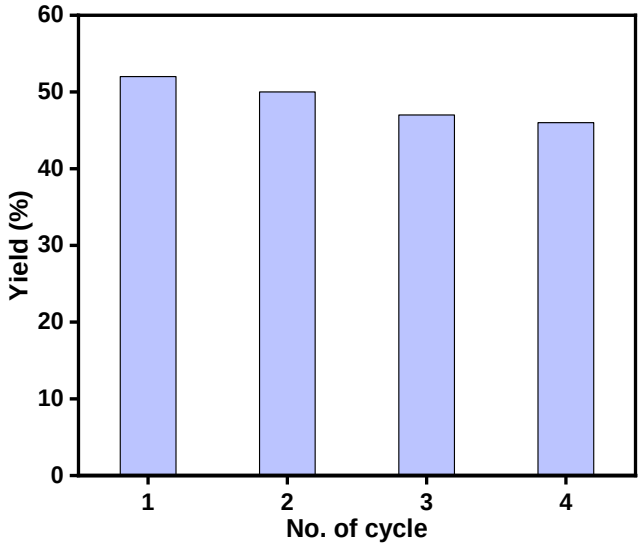

Figure S6. Isolated yields obtained during recycling of **DI-PF** in four successive photocatalytic cycles.

Table S8. Optimization of reaction conditions using various photocatalyst (PC) and diazonium salt.

Entry	Conditions (PC, 1 mol %)	Heteroarenes	Product (Yield)
1	DI-PF (without light, 24 h), 1a		No product

2	**Blue light (without PC, 24 h), 1a**		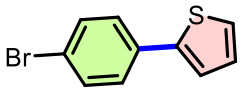 (10 %)
3	**DI-PF (TEMPO), 1a**		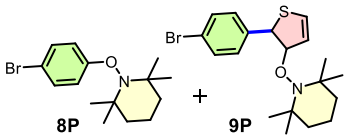 **8P** + **9P**

Table S9. Comparison table of E/Z isomerization of stilbene and heteroarylation using **DI-PF**, **DI-PI** (this work) and literature reported TADF materials.

PC	**Reaction**	**Yield** (%)	**Ref.**
This work	Isomerization	66	
	Heteroarylation	86	
4CzIPN	Isomerization	90	*J. Am. Chem. Soc.*, 2018, **140**, 13719–13725 (20)
	Heteroarylation	81	*RSC Adv.*, 2021, **11**, 14079–14084 (29)
	Heteroarylation	83	Chemistry Select, 2021, **6**, 12440–12445 (30)
Eosin Y	Heteroarylation	80	*J. Am. Chem. Soc.*, 2012, **134**, 2958–2961 (26)
pDTCz-DPmS	Isomerization	63	*J. Org. Chem.*, 2023, **88**, 6364–6373 (16)

^{1}H-NMR spectra of arylation of heteroarenes (electron transfer reactions)

^{1}H NMR spectra of 1a

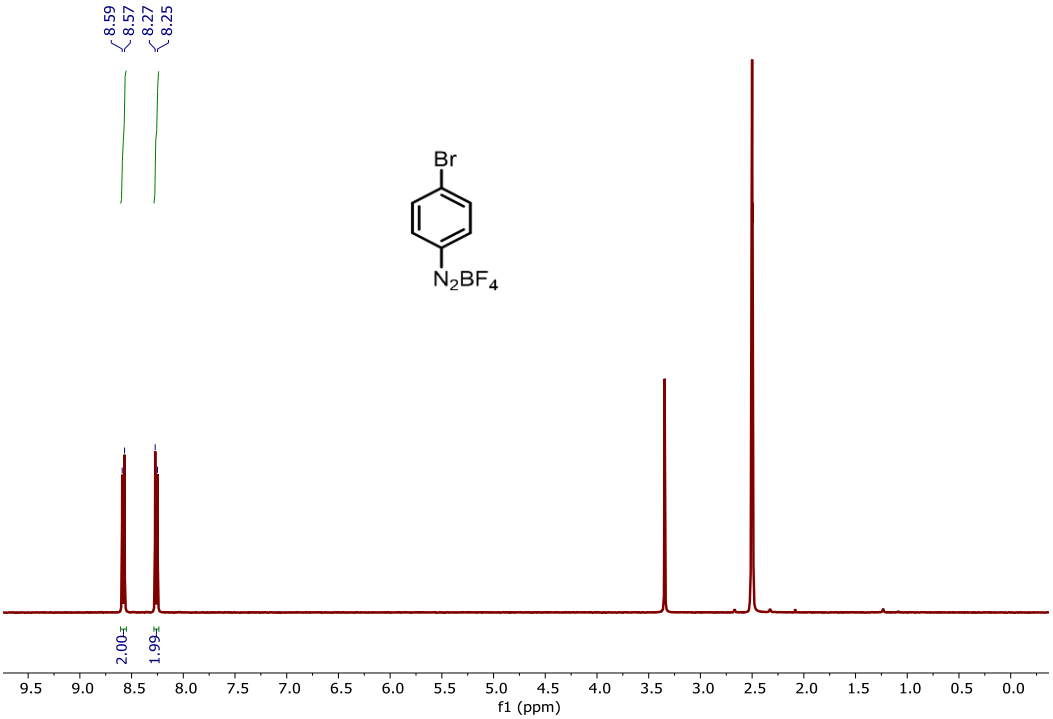

^{1}H NMR spectra of 1b

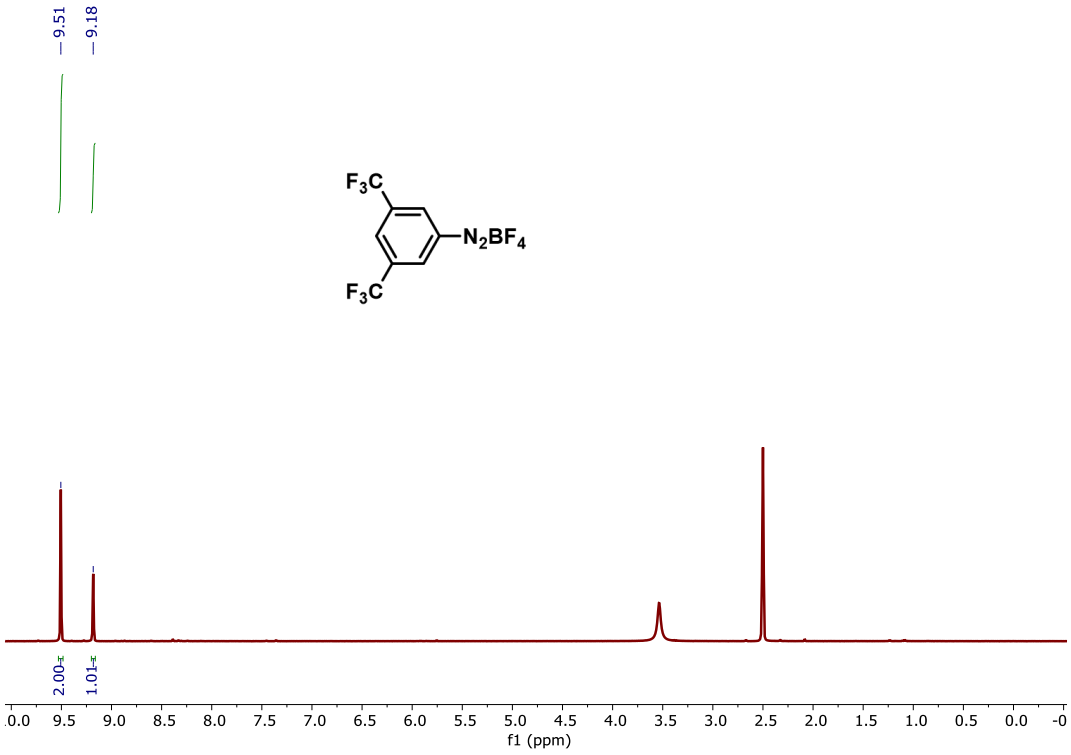

^{1}H NMR spectra of 1c

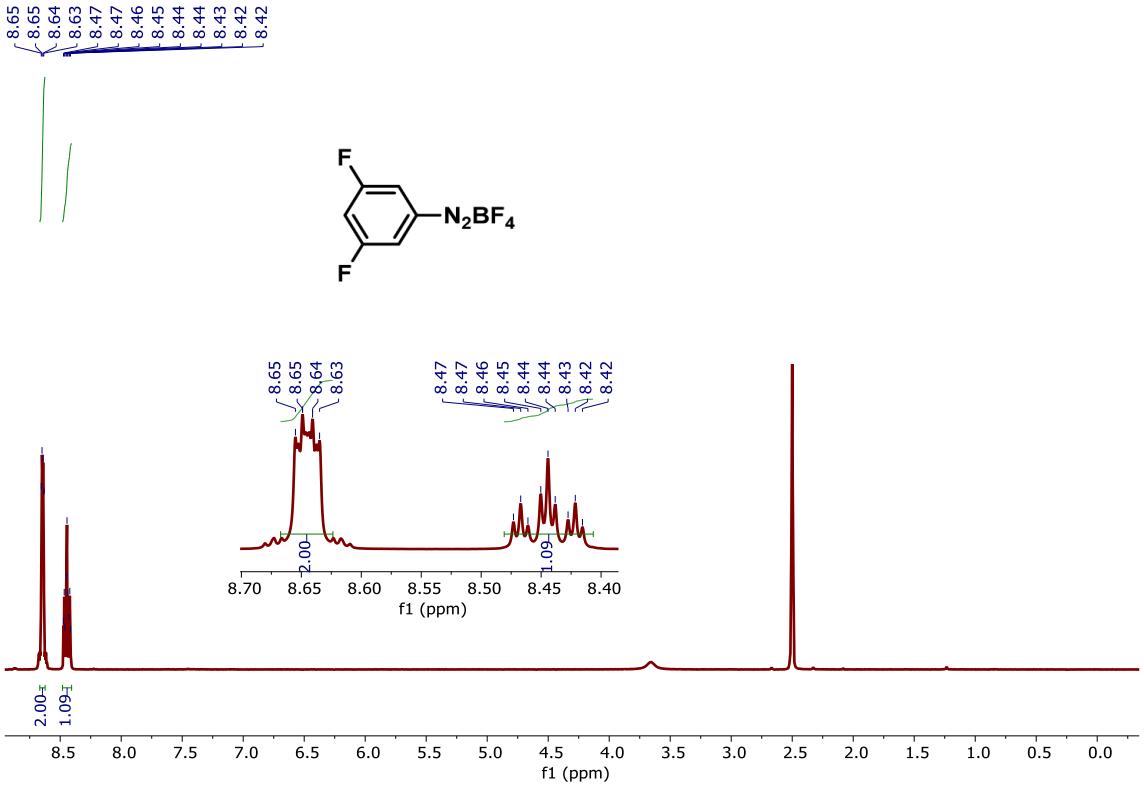

^{1}H NMR spectra of 1d

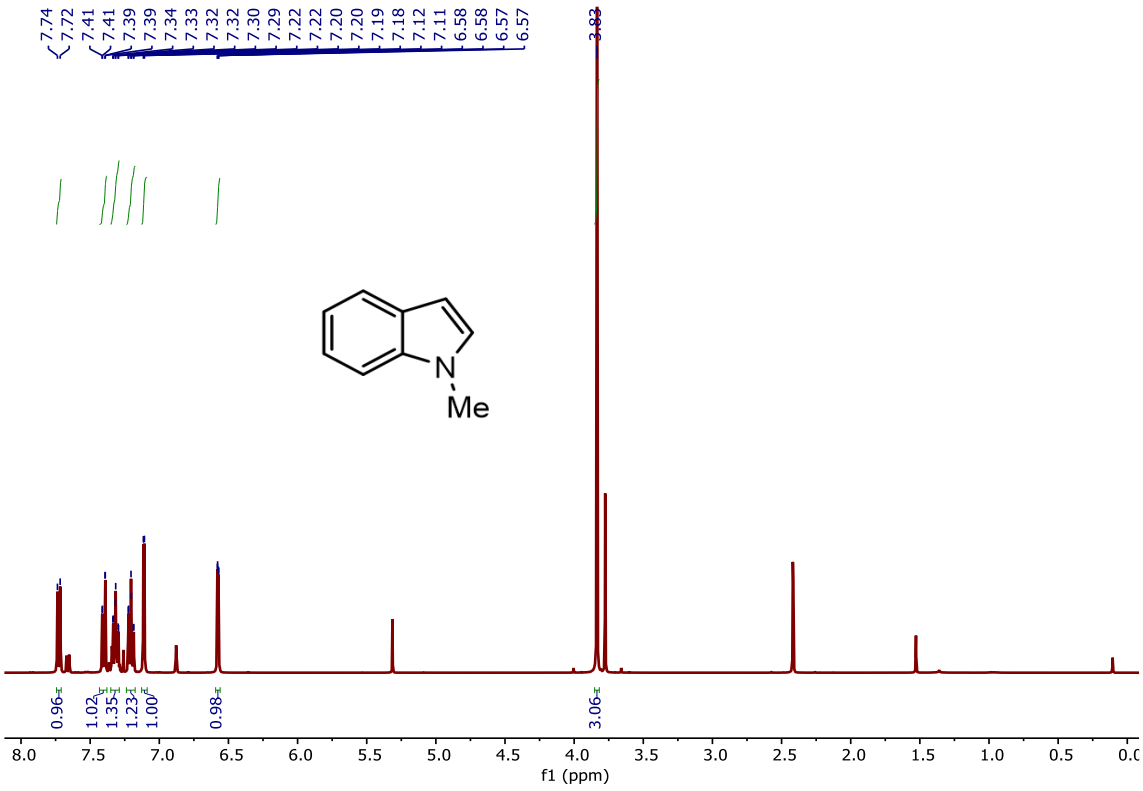

^{1}H NMR spectra of 1P

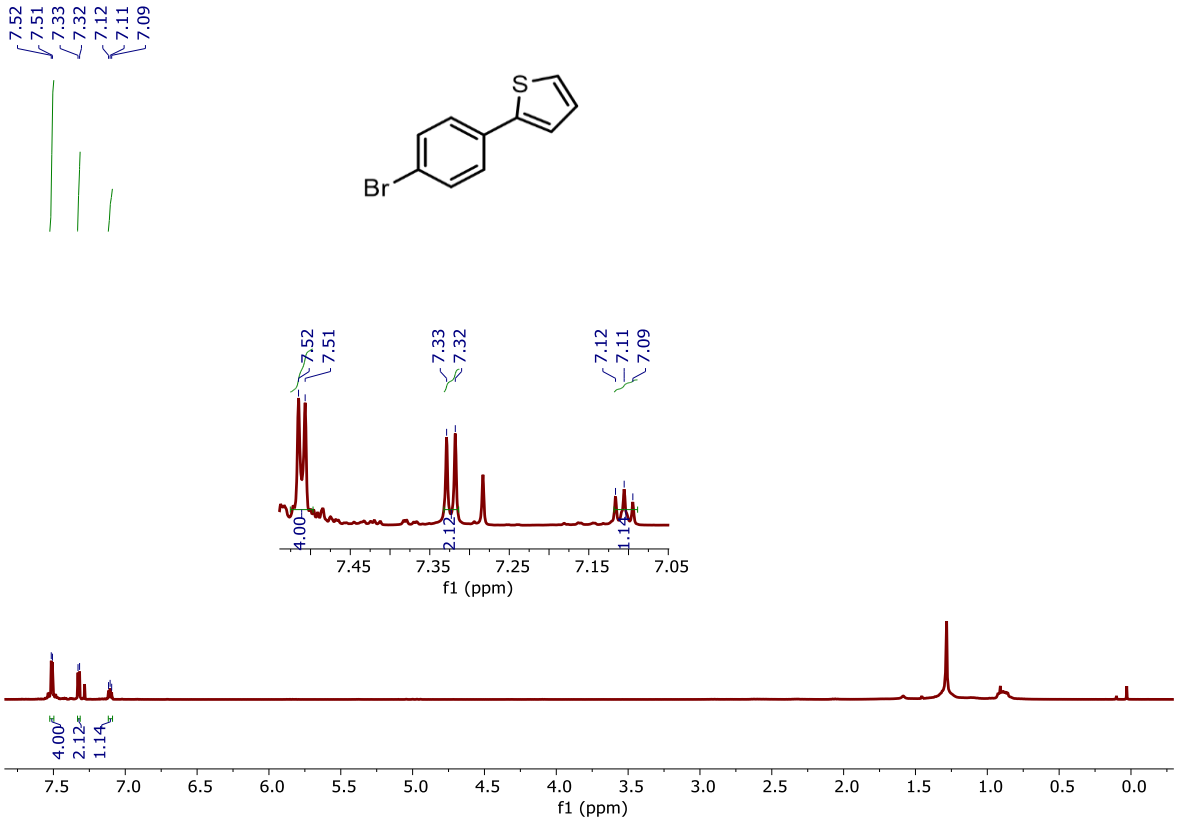

^{1}H NMR spectra of 2P

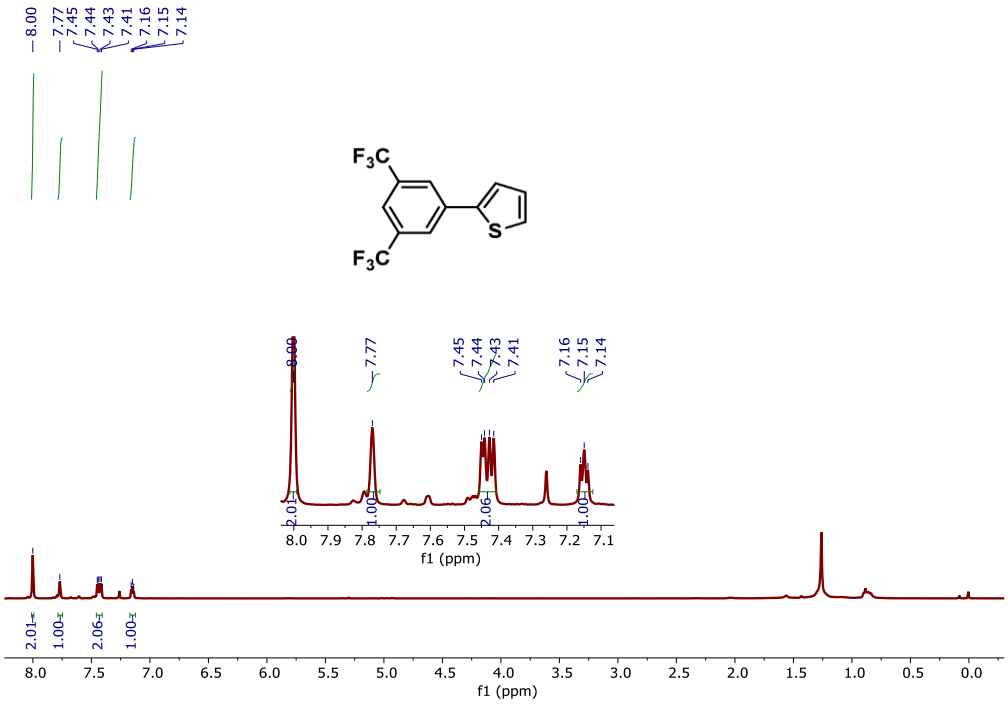

^{1}H NMR spectra of 3P

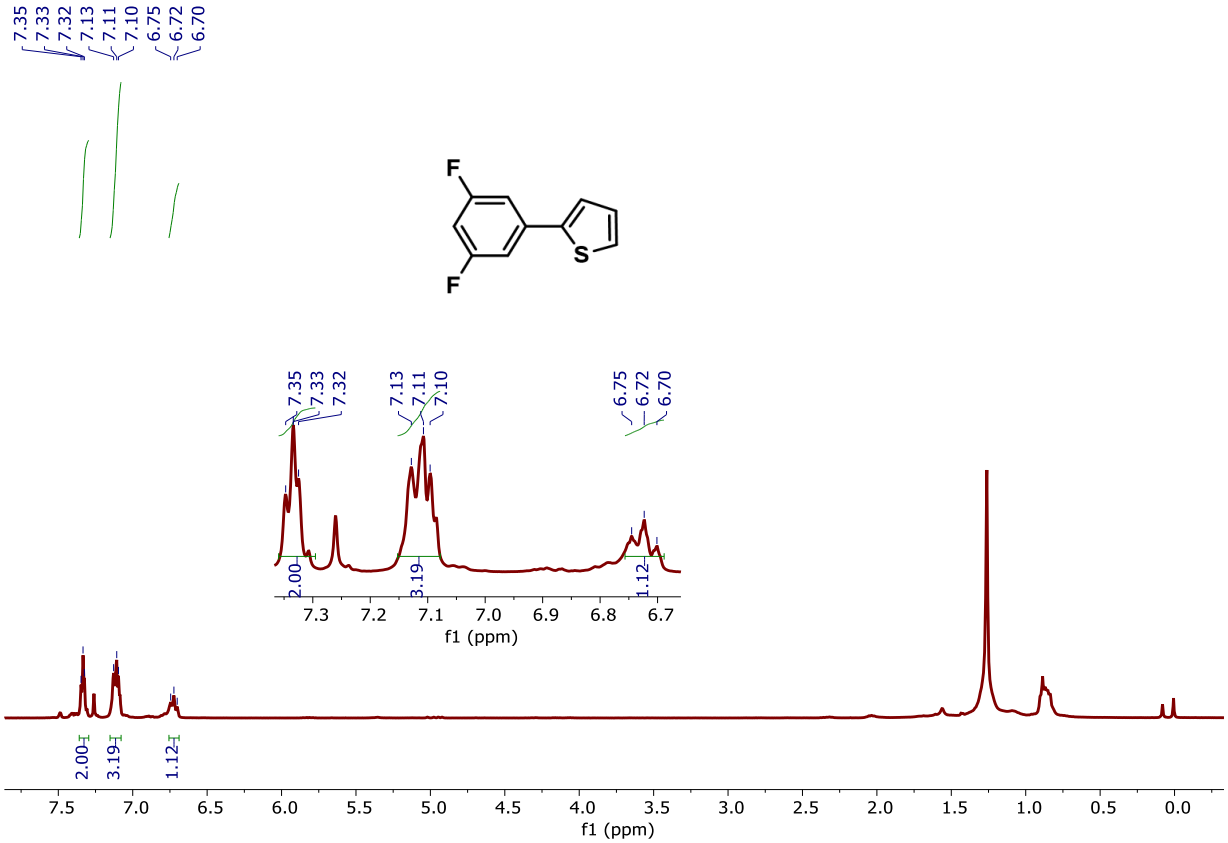

^{1}H NMR spectra of 4P

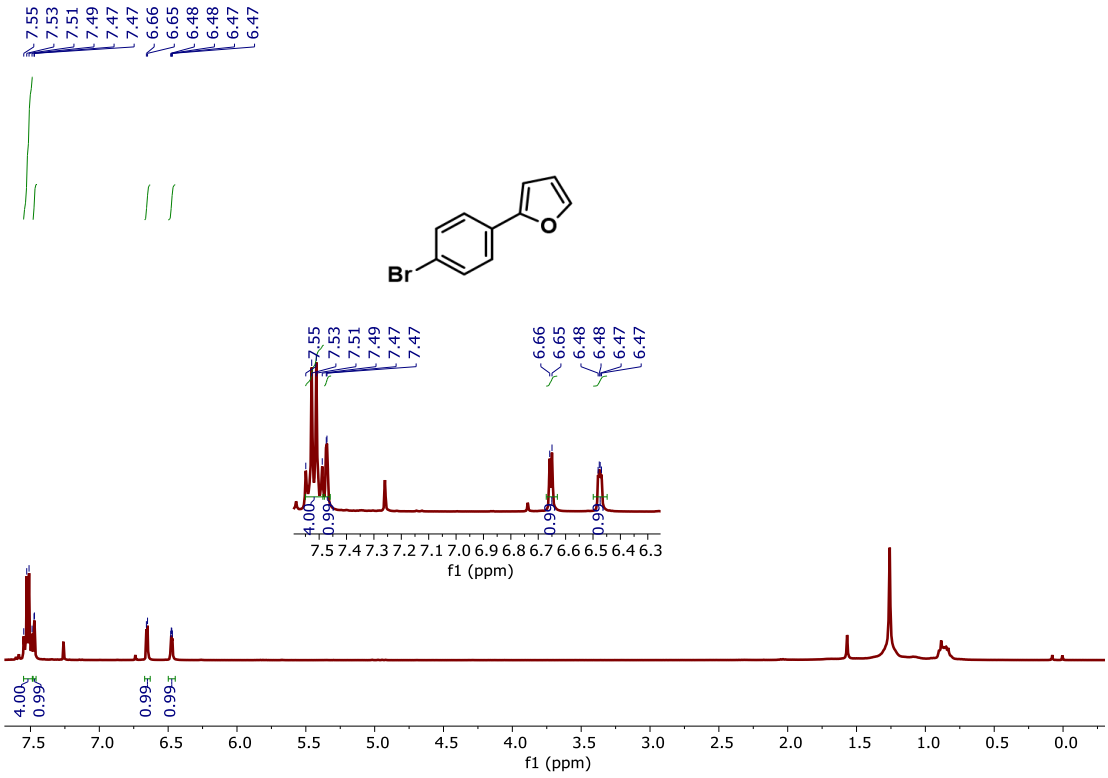

^{1}H NMR spectra of 5P

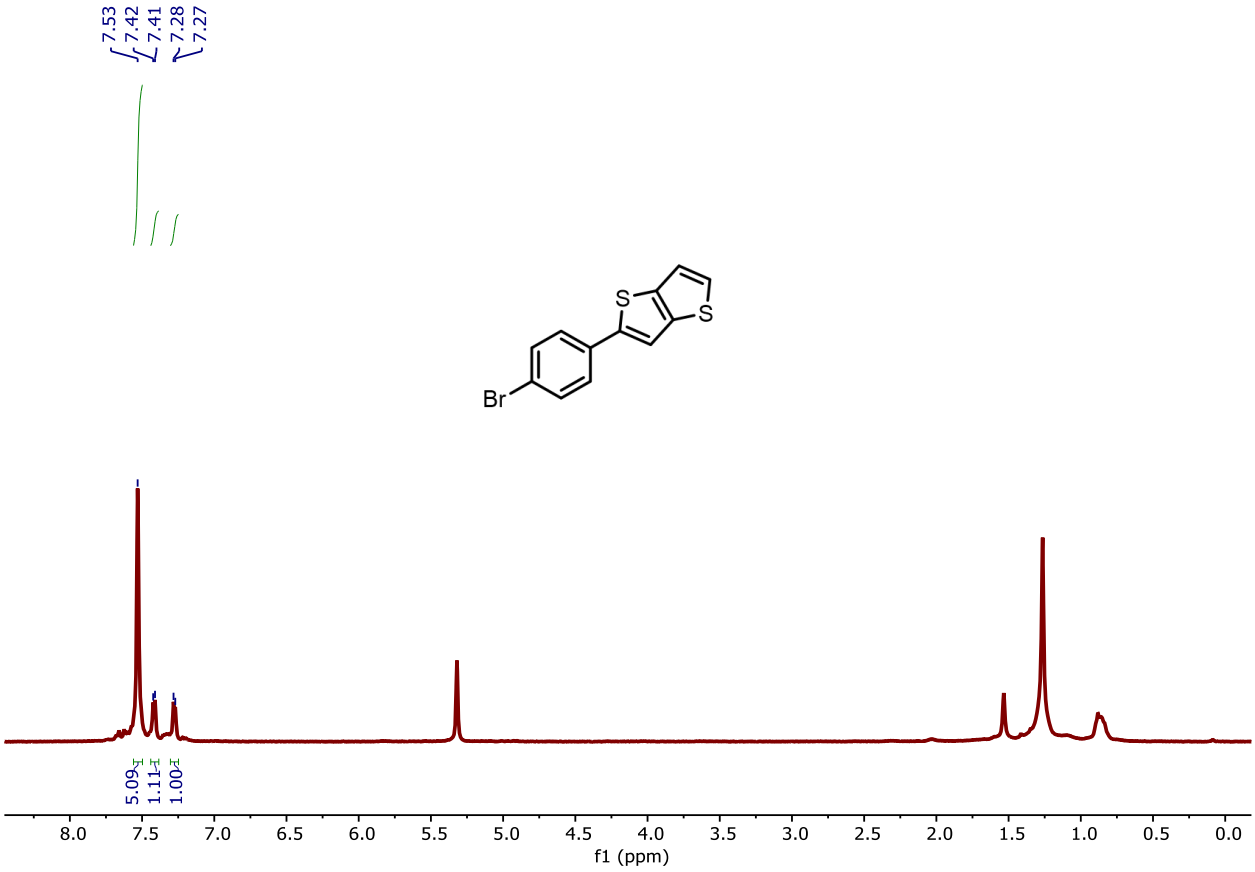

^{1}H NMR spectra of 6P

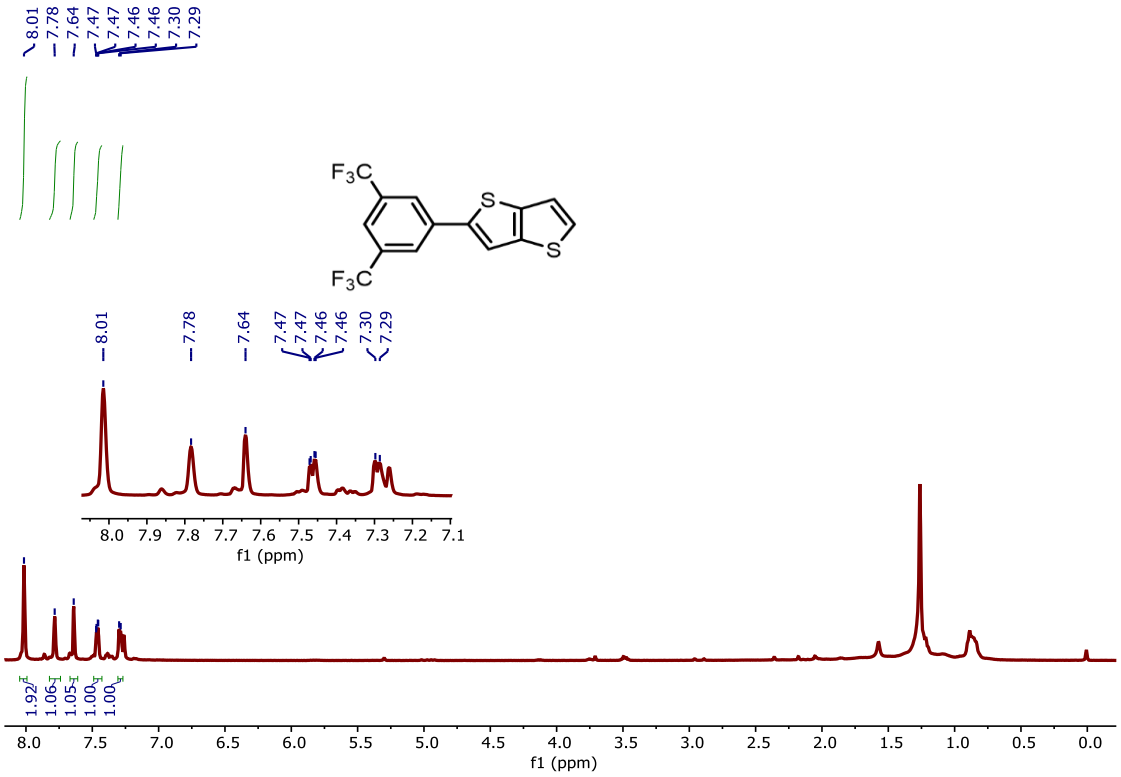

^{1}H NMR spectra of 7P

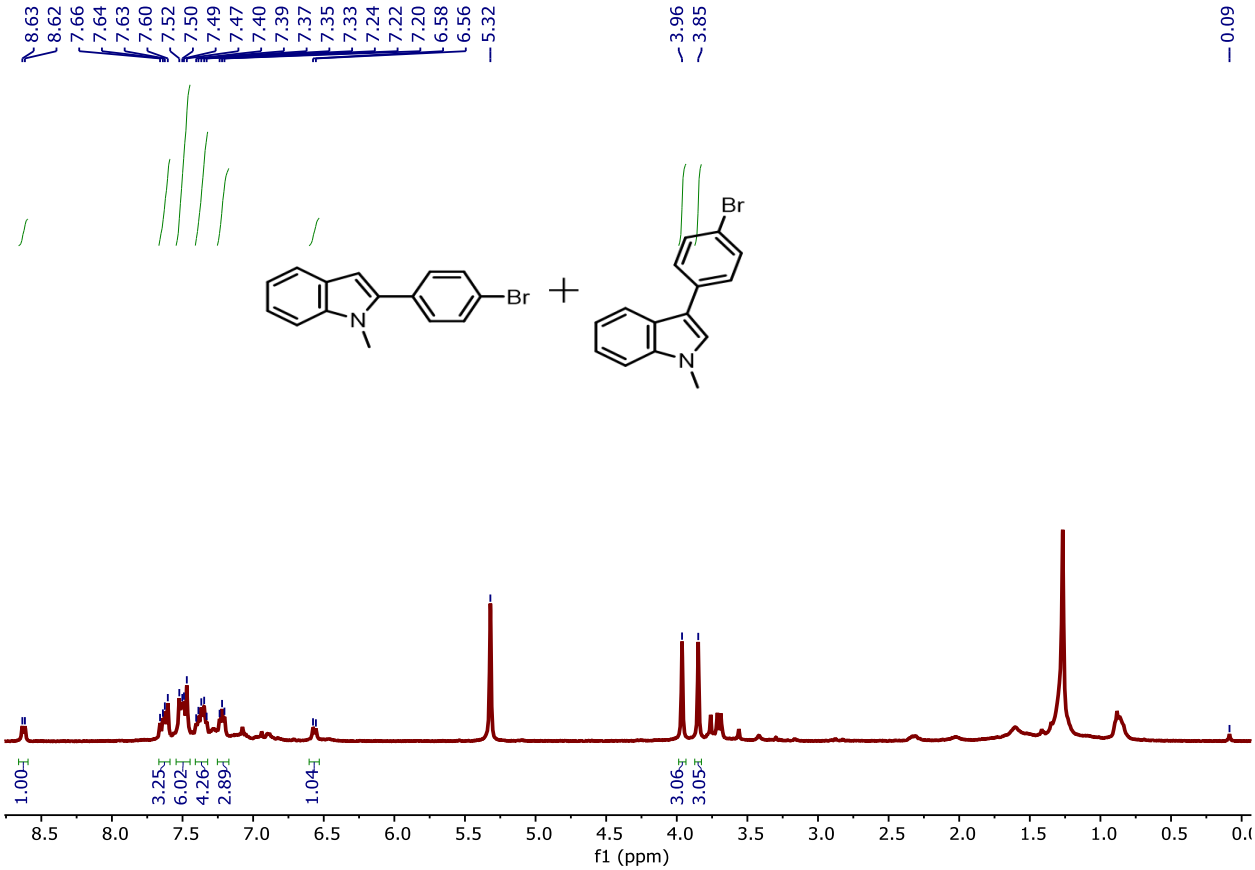

12. Frequencies and Coordinates of DFT Optimized Geometries

Table S10: Results of first three frequencies and molecular symmetries calculated from geometry optimization of **DI-PF** and **DI-PI**.

Compounds	Symmetry	First Three Frequencies
DI-PF	C_1	4.35 4.77 8.34
DI-PI	C_1	5.19 5.61 8.36

Coordinates of geometry optimized structure of DI-PF

C	5.20858	-2.41309	0.75996
C	6.59931	-2.57830	0.54060
C	7.11838	-1.27338	0.15157
C	6.04162	-0.35563	0.25995
N	4.87075	-1.06070	0.57801
C	8.36284	-0.76390	-0.29975
C	8.58729	0.62870	-0.48863
C	7.53383	1.51449	-0.14914
C	6.23516	1.04615	0.18939
C	4.37292	-3.47903	1.09655
C	4.95373	-4.72994	1.28665
C	6.33767	-4.90368	1.15013

C	7.15985	-3.84411	0.77876	C	2.51373	-0.84273	1.16881
N	7.53541	2.91256	-0.09788	C	-0.48985	0.44949	-0.75321
C	6.26286	3.34310	0.30110	C	-1.52985	0.24209	0.18869
C	5.42498	2.21678	0.49369	C	-1.22599	-0.34168	1.49658
N	9.52363	-1.45709	-0.65853	C	0.12446	-0.71095	1.81872
C	10.46742	-0.53307	-1.12369	C	-0.84129	1.01659	-1.99594
C	9.92617	0.77335	-1.04144	C	-2.14970	1.35589	-2.29795
C	5.83808	4.64907	0.55253	C	-3.17035	1.15024	-1.35281
C	4.53554	4.83592	1.00478	C	-2.85207	0.60251	-0.11769
C	3.68963	3.73842	1.21940	N	-2.21576	-0.51975	2.36499
C	4.12376	2.43894	0.97601	C	-1.91543	-1.06525	3.56129
C	11.73070	-0.79446	-1.65826	C	-0.56670	-1.43904	3.88151
C	12.47642	0.28354	-2.12412	N	0.43140	-1.25073	2.99385
C	11.95740	1.58563	-2.07394	C	-2.94900	-1.27353	4.51657
C	10.69490	1.83664	-1.54581	C	-2.63416	-1.82839	5.72494
C	3.54540	-0.65759	0.25794	C	-1.29730	-2.19905	6.04226
C	8.66990	3.76764	0.04122	C	-0.27856	-2.01415	5.15047
C	9.64250	-2.84104	-0.98995	C	-4.87062	2.88150	-1.79350
C	8.83372	4.85280	-0.82394	C	-6.26694	3.01016	-1.58669
C	9.91858	5.71529	-0.66281	C	-6.76129	1.68214	-1.24801
C	10.86212	5.51294	0.35190	C	-5.66365	0.79093	-1.37266
C	10.68226	4.41748	1.20877	N	-4.50649	1.53219	-1.65629
C	9.59580	3.55868	1.06851	C	-8.00054	1.13278	-0.83083
C	8.85597	-3.40120	-2.00141	C	-8.19915	-0.26927	-0.69388
C	9.00723	-4.74419	-2.33478	C	-7.12237	-1.12112	-1.04736
C	9.95441	-5.55318	-1.69054	C	-5.82822	-0.61623	-1.34947
C	10.74358	-4.97270	-0.68991	C	-4.05234	3.97575	-2.07859
C	10.59196	-3.63121	-0.33714	C	-4.65621	5.22044	-2.23456
C	3.25743	-0.10337	-1.00233	C	-6.04544	5.36030	-2.11263
C	1.96207	0.26133	-1.32250	C	-6.85028	4.27194	-1.78906
C	0.89175	0.07514	-0.42241	N	-7.09496	-2.51630	-1.14401
C	1.19195	-0.49477	0.84050	C	-5.80766	-2.90879	-1.53367

C	-4.98911	-1.76070	-1.67486	H	2.68213	3.90039	1.59061
N	-9.17920	1.79076	-0.46409	H	3.45878	1.61328	1.18204
C	-10.11062	0.83253	-0.04485	H	12.11050	-1.80774	-1.72131
C	-9.54237	-0.45944	-0.16534	H	13.46284	0.10922	-2.54367
C	-5.35330	-4.19788	-1.81803	H	12.54428	2.41348	-2.46058
C	-4.03911	-4.34639	-2.25003	H	10.31218	2.84668	-1.54800
C	-3.21067	-3.22699	-2.41222	H	8.12137	5.00457	-1.62848
C	-3.67451	-1.94421	-2.13681	H	10.03795	6.55271	-1.34523
C	-11.38576	1.05032	0.48093	H	11.40225	4.23635	2.00261
C	-12.11627	-0.05765	0.89809	H	9.46542	2.71816	1.74185
C	-11.57096	-1.34679	0.80929	H	8.12268	-2.78461	-2.51037
C	-10.29674	-1.55445	0.29049	H	8.38006	-5.17188	-3.11264
C	-8.20934	-3.38894	-1.32777	H	11.48134	-5.57912	-0.17113
C	-9.32625	3.15828	-0.08006	H	11.19439	-3.19475	0.45309
C	-9.12422	-3.16543	-2.36185	H	4.05977	0.04268	-1.71699
C	-10.19089	-4.04063	-2.54601	H	1.78233	0.69182	-2.30013
C	-10.36091	-5.16648	-1.72741	H	2.71298	-1.24086	2.15573
C	-9.42828	-5.38272	-0.70549	H	-0.08336	1.18587	-2.75108
C	-8.36364	-4.50454	-0.50034	H	-2.39932	1.75925	-3.27330
C	-10.28541	3.95598	-0.70919	H	-3.62076	0.43677	0.62684
C	-10.46453	5.27966	-0.30562	H	-3.96812	-0.99436	4.27740
C	-9.69351	5.83496	0.72304	H	0.73795	-2.29710	5.39627
C	-8.73588	5.01894	1.34248	H	-2.97973	3.86328	-2.18413
C	-8.55726	3.69297	0.95838	H	-4.04210	6.08529	-2.46731
F	-1.07683	-2.73664	7.25010	H	-6.50453	6.33177	-2.26948
F	-3.57176	-2.04536	6.65786	H	-7.91875	4.40881	-1.70514
H	3.30563	-3.34010	1.21978	H	-6.00934	-5.05488	-1.71909
H	4.32545	-5.57229	1.56035	H	-3.65984	-5.33864	-2.47558
H	6.77897	-5.87840	1.33536	H	-2.19246	-3.35819	-2.76613
H	8.22418	-4.00535	0.68680	H	-3.01946	-1.10194	-2.30151
H	6.50798	5.48985	0.41469	H	-11.78621	2.05321	0.57464
H	4.17952	5.84184	1.20649	H	-13.11136	0.08268	1.30983

H	-12.14631	-2.19908	1.15834
H	-9.89434	-2.55638	0.26287
H	-9.00131	-2.30104	-3.00573
H	-10.90291	-3.84821	-3.34439
H	-9.54062	-6.24378	-0.05191
H	-7.66033	-4.66780	0.30987
H	-10.87396	3.53987	-1.52058
H	-11.20981	5.89223	-0.80614
H	-8.12225	5.42723	2.14128
H	-7.81608	3.07069	1.44863
C	10.12889	-7.00113	-2.08251
H	10.69954	-7.09287	-3.01484
H	10.66604	-7.56213	-1.31285
H	9.16339	-7.49000	-2.24621
C	12.02823	6.45488	0.53486
H	12.20291	7.05451	-0.36271
H	11.84971	7.14966	1.36477
H	12.94992	5.91041	0.76301
C	-11.50505	-6.12483	-1.95781
H	-11.30008	-6.78999	-2.80571
H	-11.68143	-6.75529	-1.08195
H	-12.43384	-5.59158	-2.18370
C	-9.89802	7.26290	1.17005
H	-10.43843	7.84423	0.41792
H	-10.47867	7.30742	2.09965
H	-8.94317	7.76217	1.36236

Coordinates of geometry optimized structure of DI-PI

C	6.00395	-2.33977	1.12016
C	7.40710	-2.27281	0.92878
C	7.67147	-1.02863	0.21833
C	6.43054	-0.34786	0.10898
N	5.41270	-1.17176	0.61075
C	8.80625	-0.40850	-0.36399
C	8.75849	0.90972	-0.89736
C	7.53893	1.62224	-0.77542
C	6.34620	1.00215	-0.31437
C	5.38317	-3.43302	1.72647
C	6.19199	-4.45495	2.21560
C	7.58723	-4.37736	2.10595
C	8.19730	-3.30132	1.46844
N	7.26408	2.96099	-1.07541
C	5.91703	3.21328	-0.78136
C	5.31018	2.02525	-0.30398
N	10.09356	-0.92244	-0.55526
C	10.85267	0.02737	-1.24998
C	10.06145	1.17802	-1.48827
C	5.23432	4.42866	-0.85922
C	3.90352	4.45664	-0.45395
C	3.28195	3.29917	0.03596
C	3.97211	2.09379	0.12006
C	12.16090	-0.09975	-1.72143
C	12.69534	0.95618	-2.45278
C	11.92795	2.09903	-2.72134
C	10.62265	2.21498	-2.25351
C	4.04271	-1.13107	0.22756
C	8.20368	4.03166	-1.16282
C	10.49382	-2.29285	-0.53453
C	8.18314	4.88776	-2.26705
C	9.06883	5.96415	-2.33161
C	9.99600	6.20327	-1.31013
C	9.99959	5.33546	-0.20836
C	9.11114	4.26744	-0.12456
C	9.86704	-3.23063	-1.36150

C	10.29139	-4.55611	-1.35383	C	-4.20629	1.80810	-0.44389
C	11.35784	-4.97578	-0.54529	N	-9.00351	-0.84080	-1.68634
C	11.98363	-4.02122	0.26555	C	-9.84412	-0.10946	-0.83438
C	11.55847	-2.69204	0.27705	C	-9.06530	0.80093	-0.07778
C	3.69555	-0.99506	-1.13249	C	-4.19646	3.90306	0.86307
C	2.36909	-0.98421	-1.51747	C	-2.84106	4.04456	0.58344
C	1.31852	-1.12535	-0.58075	C	-2.17510	3.10450	-0.21677
C	1.68875	-1.27874	0.78359	C	-2.84374	1.99927	-0.73434
C	3.04088	-1.26921	1.17535	C	-11.23040	-0.20345	-0.69743
C	-0.09681	-1.11261	-0.96026	C	-11.84482	0.58480	0.27113
C	-1.13553	-1.26706	0.02118	C	-11.08663	1.43927	1.08432
C	-0.70282	-1.43890	1.38265	C	-9.71016	1.55476	0.91706
C	0.63770	-1.42784	1.74796	C	-7.16960	3.49866	0.77424
C	-0.49363	-0.93822	-2.30423	C	-9.51027	-1.49945	-2.84484
C	-1.82136	-0.91196	-2.68791	C	-7.29639	3.92954	2.09704
C	-2.82924	-1.06454	-1.72069	C	-8.18394	4.96204	2.40483
C	-2.48574	-1.24514	-0.39088	C	-8.96206	5.57423	1.41477
C	-4.71547	-2.19137	-2.81063	C	-8.81558	5.12945	0.09298
C	-6.13014	-2.16545	-2.73390	C	-7.92452	4.11052	-0.23144
C	-6.47946	-0.97649	-1.96825	C	-10.34391	-2.61421	-2.71024
C	-5.26012	-0.34794	-1.59391	C	-10.86877	-3.23399	-3.84431
N	-4.19448	-1.08444	-2.12722	C	-10.56998	-2.76918	-5.13122
C	-7.68560	-0.41243	-1.47899	C	-9.72664	-1.65513	-5.24730
C	-7.69206	0.65333	-0.53984	C	-9.21026	-1.01644	-4.12324
C	-6.46180	1.31355	-0.29235	C	10.97827	7.34711	-1.39583
C	-5.22936	0.84604	-0.82988	C	11.82399	-6.41211	-0.56633
C	-4.01196	-3.22711	-3.42900	C	-9.94845	6.66494	1.75854
C	-4.74393	-4.26462	-3.99818	C	-11.15321	-3.43149	-6.35659
C	-6.14403	-4.27061	-3.92822	N	-1.39575	-1.61634	2.58637
C	-6.83729	-3.24081	-3.29911	C	-0.42737	-1.68531	3.59353
N	-6.22118	2.47861	0.44215	N	0.79016	-1.57669	3.10068
C	-4.85876	2.78846	0.34451	C	-2.81076	-1.56553	2.78954

C	-0.68844	-1.83756	5.03565	H	12.80941	-4.32119	0.90530
C	-3.60729	-2.67958	2.49280	H	12.03682	-1.96314	0.92339
C	-4.98281	-2.63779	2.70495	H	4.48099	-0.89271	-1.87297
C	-5.54928	-1.48212	3.22849	H	2.15020	-0.87343	-2.57272
C	-1.75869	-2.57545	5.56782	H	3.27878	-1.35253	2.22927
C	-1.91441	-2.69837	6.94789	H	0.25894	-0.80481	-3.07152
C	-1.00667	-2.09399	7.81758	H	-2.09538	-0.75511	-3.72552
C	0.06958	-1.37112	7.29772	H	-3.28211	-1.35429	0.33004
C	0.22975	-1.24462	5.92152	H	-2.92841	-3.23023	-3.45393
C	-4.77137	-0.35746	3.53746	H	-4.22132	-5.08069	-4.48834
C	-3.38808	-0.40702	3.30291	H	-6.70090	-5.09475	-4.36409
F	-6.86592	-1.43709	3.45100	H	-7.91397	-3.29085	-3.23963
C	-5.38240	0.81509	4.08229	H	-4.72768	4.64012	1.45390
N	-5.86119	1.77321	4.53404	H	-2.30122	4.90106	0.97620
H	4.30569	-3.48183	1.82748	H	-1.12286	3.24253	-0.44711
H	5.73275	-5.31021	2.70233	H	-2.30949	1.31426	-1.37590
H	8.20506	-5.16678	2.52355	H	-11.81005	-0.87575	-1.31904
H	9.27522	-3.26417	1.40443	H	-12.92083	0.52300	0.40481
H	5.73079	5.32608	-1.20972	H	-11.57772	2.02271	1.85730
H	3.34914	5.38903	-0.50585	H	-9.15032	2.21710	1.56138
H	2.24809	3.34184	0.36564	H	-6.72043	3.44719	2.88020
H	3.47429	1.22798	0.53084	H	-8.27646	5.28856	3.43728
H	12.73527	-1.00005	-1.53563	H	-9.40275	5.59303	-0.69563
H	13.71107	0.88434	-2.83043	H	-7.81276	3.78107	-1.25919
H	12.35311	2.90547	-3.31147	H	-10.55766	-3.00378	-1.72043
H	10.04799	3.09522	-2.50199	H	-11.51116	-4.10261	-3.72515
H	7.48234	4.69926	-3.07397	H	-9.47407	-1.27682	-6.23447
H	9.04267	6.62294	-3.19563	H	-8.56359	-0.15175	-4.22839
H	10.70468	5.50355	0.60164	H	10.67631	8.07862	-2.15036
H	9.11825	3.60902	0.73757	H	11.06944	7.86798	-0.43721
H	9.04373	-2.91742	-1.99471	H	11.97981	6.98998	-1.66484
H	9.78709	-5.27850	-1.99044	H	10.97905	-7.10689	-0.52247

H	12.37782	-6.63575	-1.48626	H	-3.14268	-3.57387	2.09109
H	12.48491	-6.63060	0.27682	H	-5.62108	-3.48298	2.47535
H	-9.71277	7.12900	2.72024	H	-2.46033	-3.07549	4.91164
H	-9.95814	7.45041	0.99623	H	-2.74468	-3.27657	7.34236
H	-10.96904	6.26850	1.82638	H	-1.13339	-2.18985	8.89175
H	-11.46835	-4.45722	-6.14539	H	0.78510	-0.90200	7.96636
H	-12.03338	-2.88680	-6.72019	H	1.06568	-0.69167	5.50841
H	-10.43028	-3.46144	-7.17760	H	-2.77285	0.45679	3.52479

13. References:

S1. Gaussian 09, Revision C.01, M. J. Frisch, G. W. Trucks, H. B. Schlegel, G. E. Scuseria, M. A. Robb, J. R. Cheeseman, G. Scalmani, V. Barone, B. Mennucci, G. A. Petersson, H. Nakatsuji, M. Caricato, X. Li, H. P. Hratchian, A. F. Izmaylov, J. Bloino, G. Zheng, J. L. Sonnenberg, M. Hada, M. Ehara, K. Toyota, R. Fukuda, J. Hasegawa, M. Ishida, T. Nakajima, Y. Honda, O. Kitao, H. Nakai, T. Vreven, J. A. Montgomery, Jr., J. E. Peralta, F. Ogliaro, M. Bearpark, J. J. Heyd, E. Brothers, K. N. Kudin, V. N. Staroverov, T. Keith, R. Kobayashi, J. Normand, K. Raghavachari, A. Rendell, J. C. Burant, S. S. Iyengar, J. Tomasi, M. Cossi, N. Rega, J. M. Millam, M. Klene, J. E. Knox, J. B. Cross, V. Bakken, C. Adamo, J. Jaramillo, R. Gomperts, R. E. Stratmann, O. Yazyev, A. J. Austin, R. Cammi, C. Pomelli, J. W. Ochterski, R. L. Martin, K. Morokuma, V. G. Zakrzewski, G. A. Voth, P. Salvador, J. J. Dannenberg, S. Dapprich, A. D. Daniels, O. Farkas, J. B. Foresman, J. V. Ortiz, J. Cioslowski, and D. J. Fox, Gaussian, Inc., Wallingford CT, 2010**.**

S2. A. E. Sadak, E. Karakuş, Y. M. Chumakov, N. A. Dogan, C. T. Yavuz, *ACS Appl. Energy Mater.* 2020, **3** (5), 4983–4994.

S3. S. J. Yoon, J. H. Kim, W. J. Chung and J. Y. Lee, *Chem. Eur. J.*, 2021, **27**, 3065–3073.

S4. B. Sk, S. Khodia and A. Patra, *Chem. Commun.*, 2018, **54**, 1786–1789.

S5. S. Wang, Y. Miao, X. Yan, K. Ye and Y. Wang, *J. Mater. Chem. C*, 2018, **6**, 6698–6704.

S6. W. Qin, Z. Yang, Y. Jiang, J. W. Y. Lam, G. Liang, H. S. Kwok and B. Z. Tang, *Chem. Mater.*, 2015, **27**, 3892–3901.

S7. D. H. Ahn, H. Lee, S. W. Kim, D. Karthik, J. Lee, H. Jeong, J. Y. Lee and J. H. Kwon, *ACS Appl. Mater. Interfaces*, 2019, **11**, 14909–14916.

S8. D. Thakur, D. K. Dubey, R. A. K. Yadav, M. Venkateswarulu, S. Banik, J. H. Jou and S. Ghosh, *J. Mater. Chem. C*, 2019, **8**, 228–239.

S9. S. Sharma, S. Srinivas, S. Rakshit, S. Sengupta, *Org. Biomol. Chem.* 2022, **20** (47), 9422–9430.

S10. M. A. Bryden and E. Zysman-Colman, *Chem. Soc. Rev.*, 2021, **50**, 7587–7680.

S11. D. P. Hari, P. Schroll and B. König, *J. Am. Chem. Soc.*, 2012, **134**, 2958–2961.